# The $^{12}C(\alpha,\gamma)^{16}O$ reaction

James deBoer (Notre Dame) and Marialuisa Aliotta (Edinburgh)

The Big-Three Reactions Workshop, May 29, 2024

# Motivation

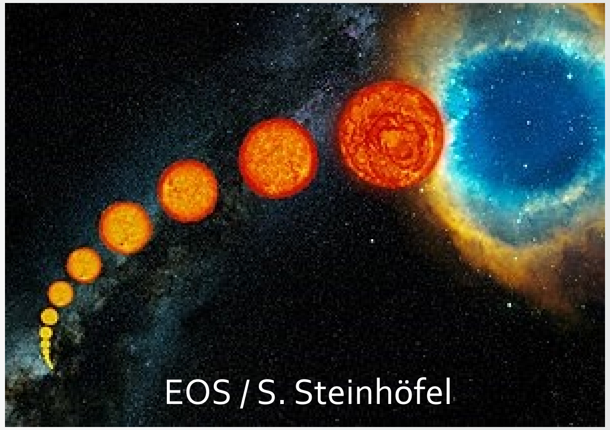
EOS / S. Steinhöfel

- Together with the 3$\alpha$ process, the $^{12}C(\alpha,\gamma)^{16}O$ reaction determines the $^{12}C/^{16}O$ ratio in the universe.
- For stellar evolution, the $^{12}C/^{16}O$ ratio determines the evolution of massive stars, which in turn effects all later stages of nucleosynthesis.

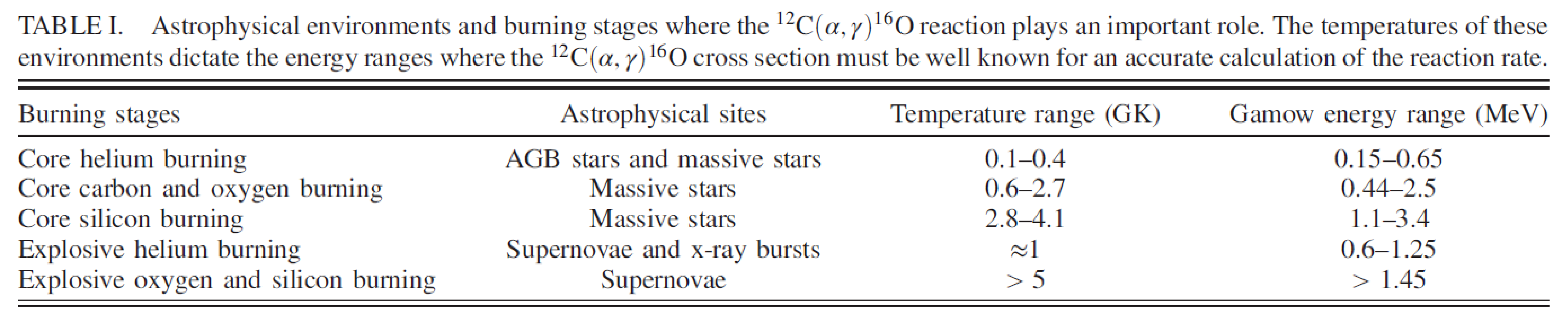
TABLE I. Astrophysical environments and burning stages where the $^{12}C(\alpha,\gamma)^{16}O$ reaction plays an important role. The temperatures of these environments dictate the energy ranges where the $^{12}C(\alpha,\gamma)^{16}O$ cross section must be well known for an accurate calculation of the reaction rate.

| Burning stages | Astrophysical sites | Temperature range (GK) | Gamow energy range (MeV) |
|---|---|---|---|
| Core helium burning | AGB stars and massive stars | 0.1–0.4 | 0.15–0.65 |
| Core carbon and oxygen burning | Massive stars | 0.6–2.7 | 0.44–2.5 |
| Core silicon burning | Massive stars | 2.8–4.1 | 1.1–3.4 |
| Explosive helium burning | Supernovae and x-ray bursts | $\approx 1$ | 0.6–1.25 |
| Explosive oxygen and silicon burning | Supernovae | $> 5$ | $> 1.45$ |

# Motivation Highlight: Black Hole Mass Gap
# **Link to LIGO**

- **Farmer *et al.* (2020), Mehta *et al.* (2022)**

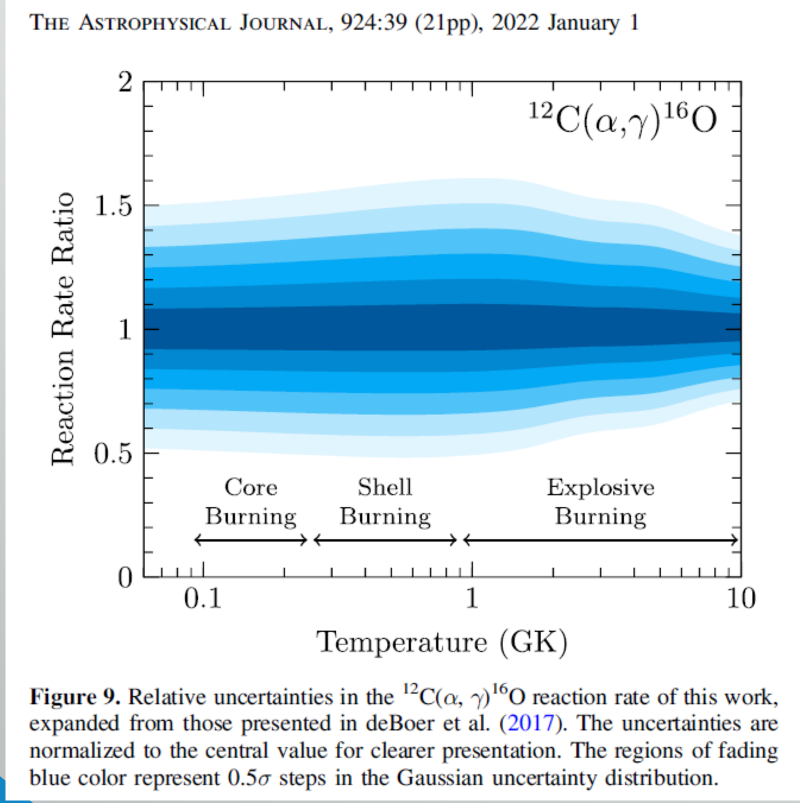

THE ASTROPHYSICAL JOURNAL, 924:39 (21pp), 2022 January 1

**Figure 9.** Relative uncertainties in the $^{12}C(\alpha, \gamma)^{16}O$ reaction rate of this work, expanded from those presented in deBoer et al. (2017). The uncertainties are normalized to the central value for clearer presentation. The regions of fading blue color represent 0.5$\sigma$ steps in the Gaussian uncertainty distribution.

Following Gialanella *et al.* (2001)

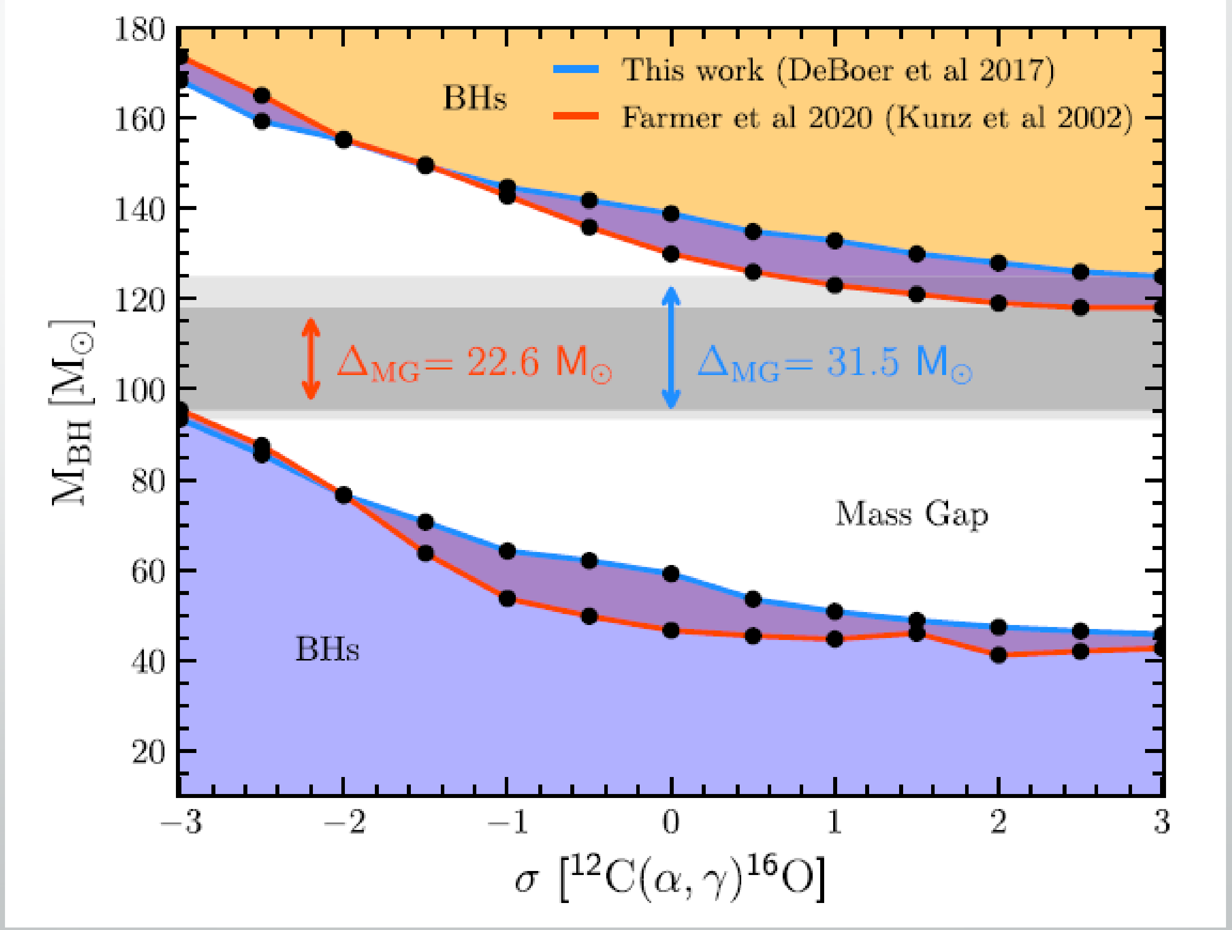

# Motivation Highlight: White Dwarf Seismology

- **Chidester *et al*. (2022,2023)**

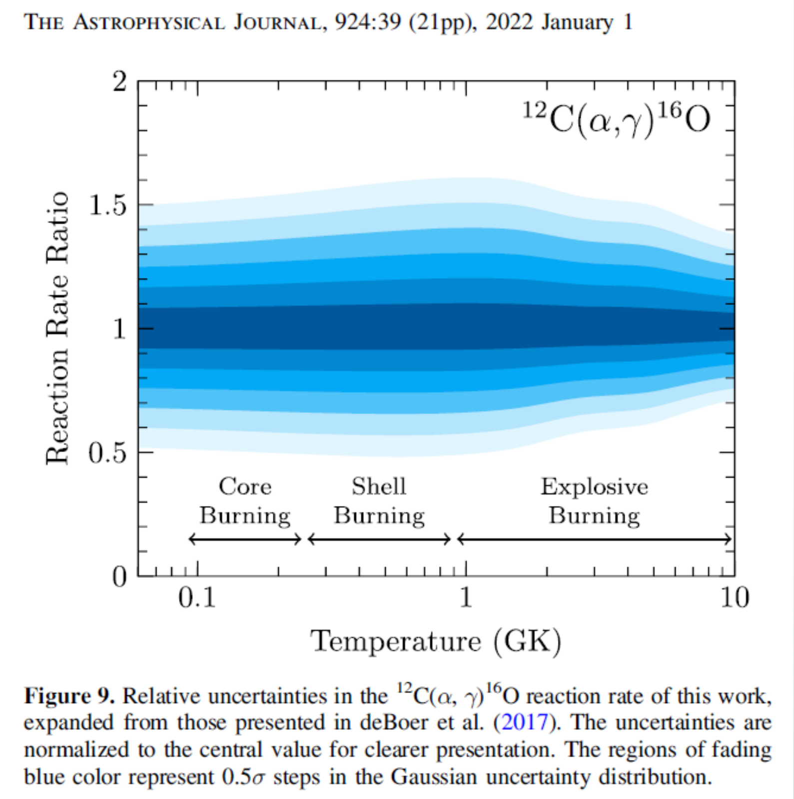

THE ASTROPHYSICAL JOURNAL, 924:39 (21pp), 2022 January 1

**Figure 9.** Relative uncertainties in the $^{12}$C$(\alpha, \gamma)^{16}$O reaction rate of this work, expanded from those presented in deBoer et al. (2017). The uncertainties are normalized to the central value for clearer presentation. The regions of fading blue color represent 0.5$\sigma$ steps in the Gaussian uncertainty distribution.

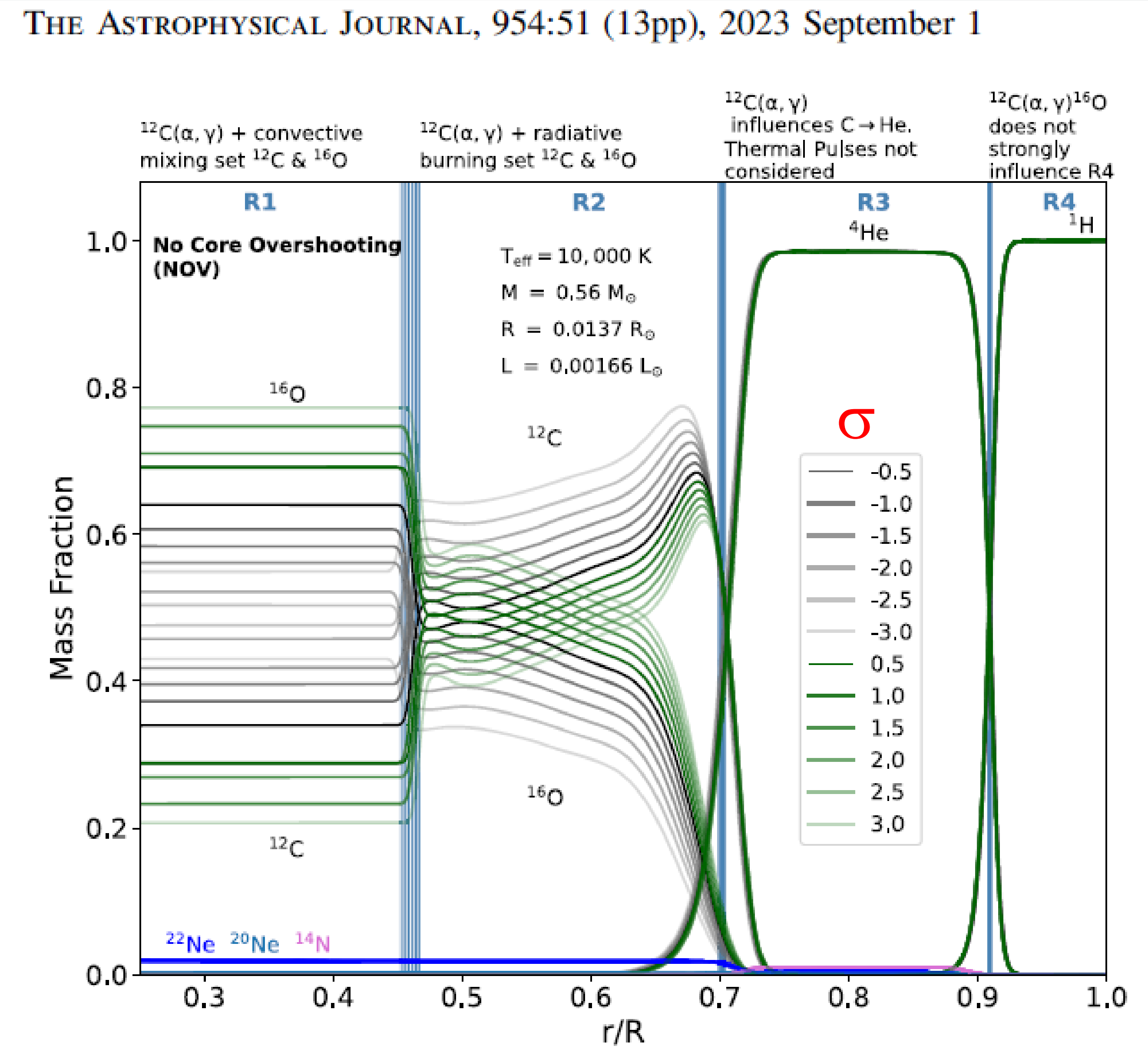

THE ASTROPHYSICAL JOURNAL, 954:51 (13pp), 2023 September 1

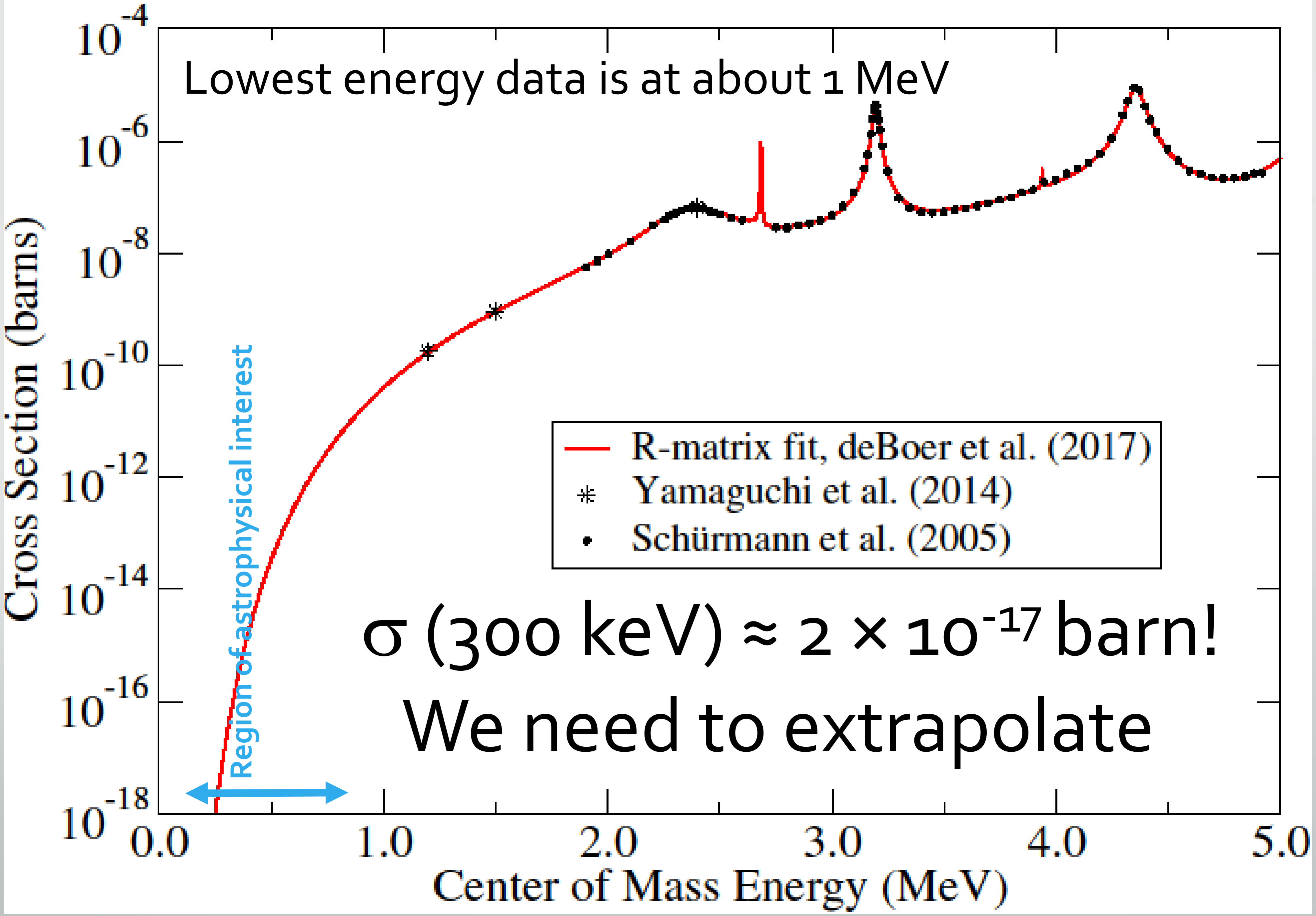

Lowest energy data is at about 1 MeV

$\sigma$ (300 keV) ≈ 2 × $10^{-17}$ barn!

We need to extrapolate

# $^{12}C(\alpha,\gamma)^{16}O$ S-factor

$$S(E) = \sigma(E)Ee^{2\pi\eta}$$

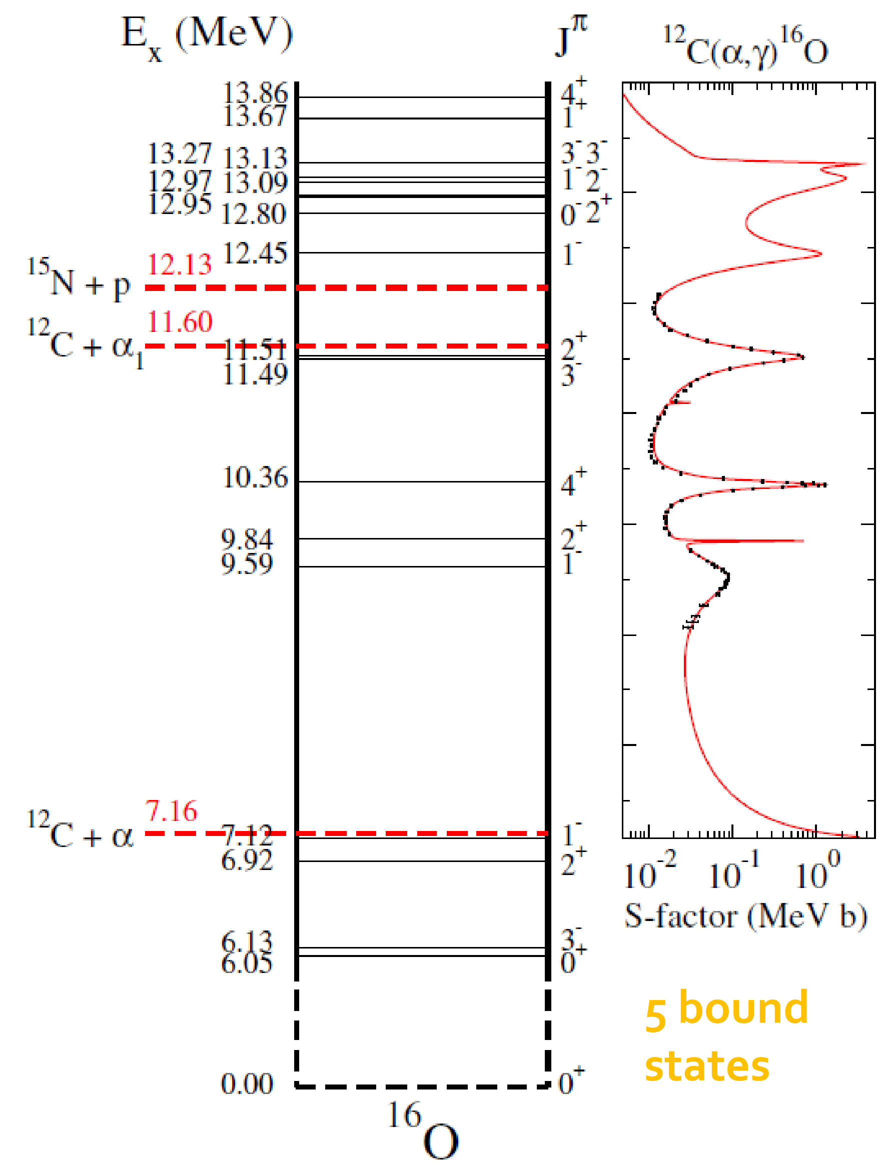

5 bound states

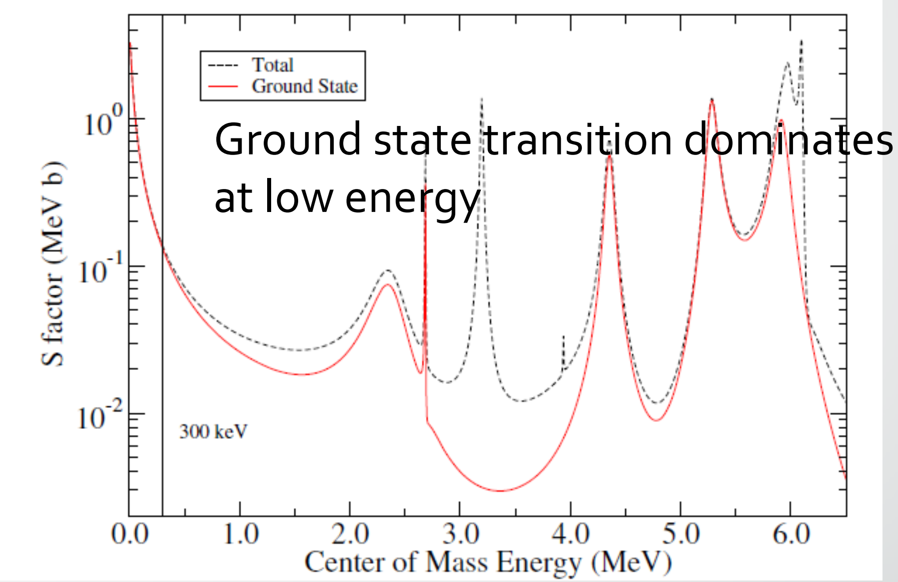

Ground state transition dominates at low energy

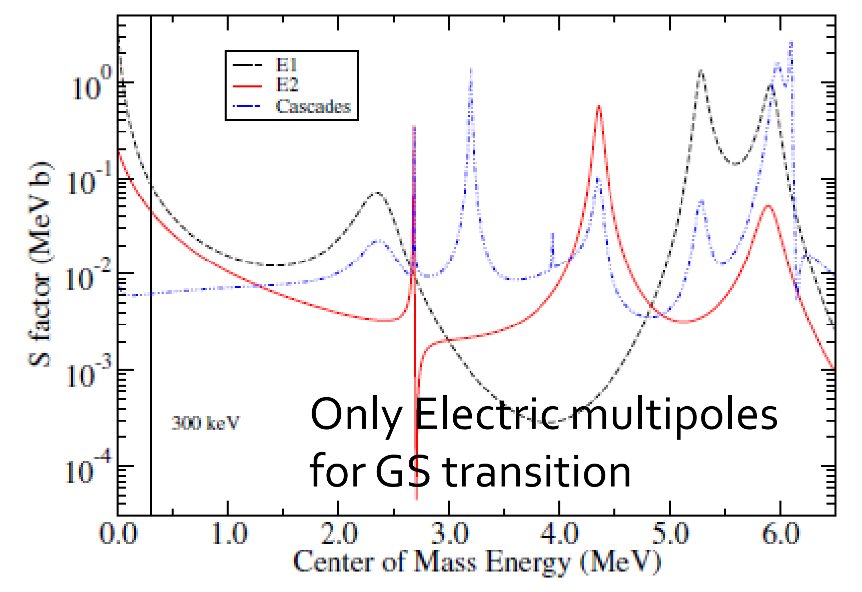

Only Electric multipoles for GS transition

# “World Data Set” for the ground state transition

- In hindsight, it was not the best idea to only report “E1 and E2” cross sections, since this makes it harder to understand discrepancies between the different measurements

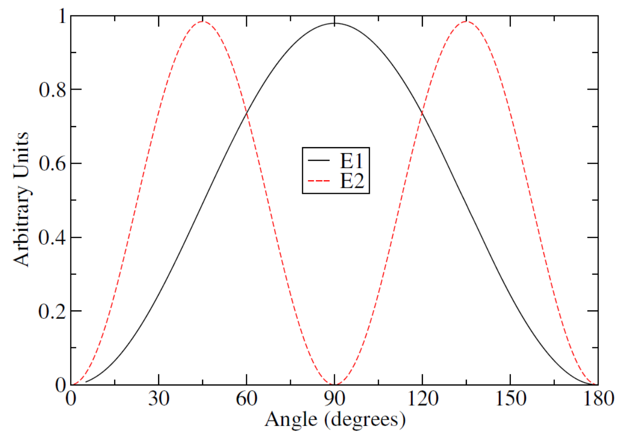

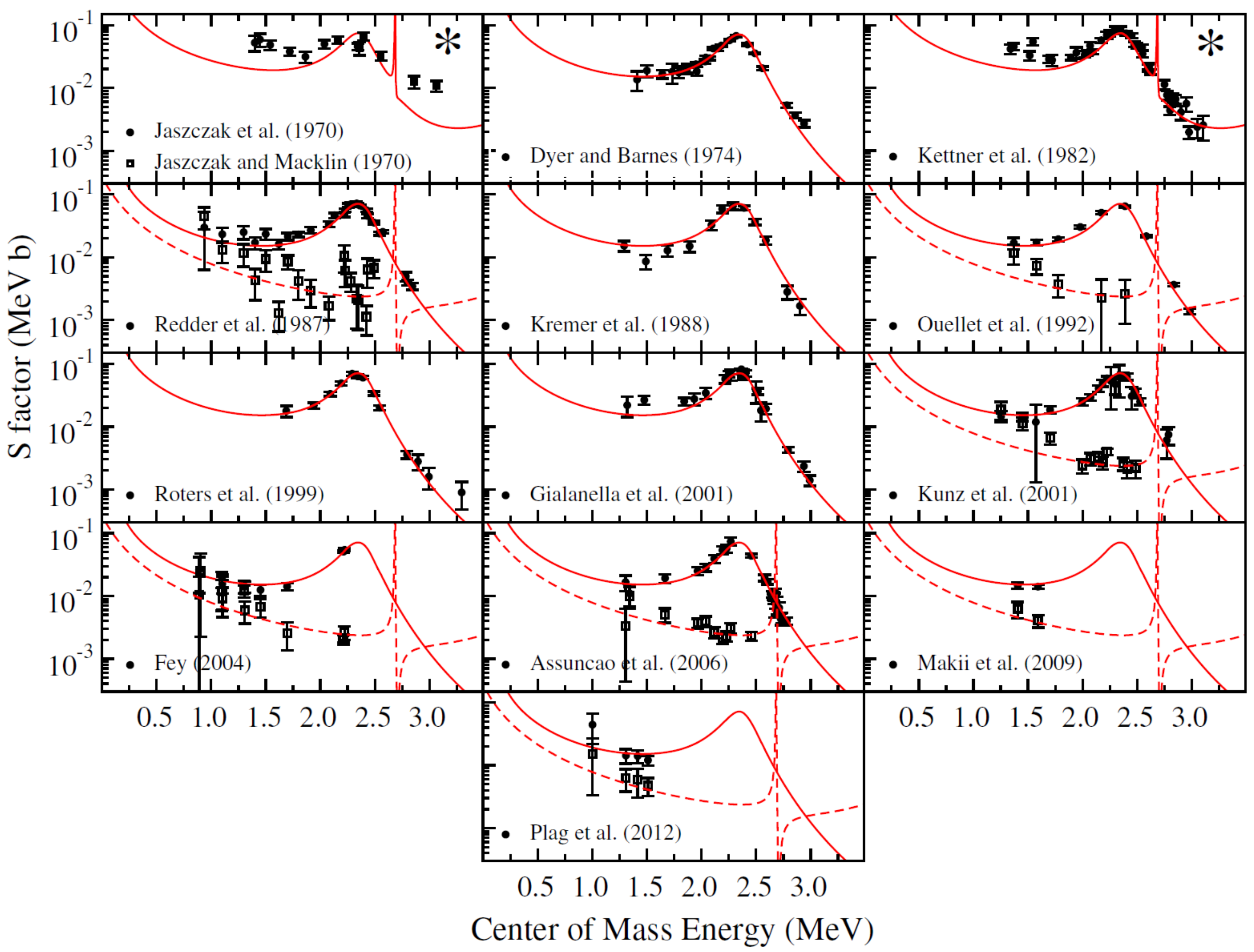

# Major experimental challenges

- Very low cross section
- Background reactions
  - $^{13}C(\alpha,n)^{16}O$
  - High Q-value $(n,\gamma)$ on nearby material
- Inverse kinematics has issues
- Solutions
  - Very clean target / beam lines
  - Time-of-flight method to separate prompt $\gamma$-ray signals from $(n,\gamma)$ delayed ones
  - Recoil separators
  - More exotic solutions

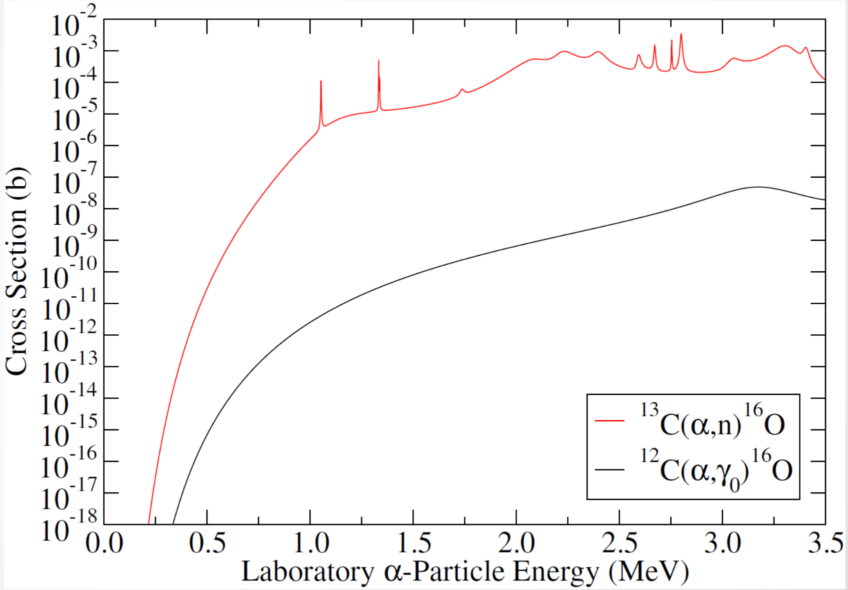

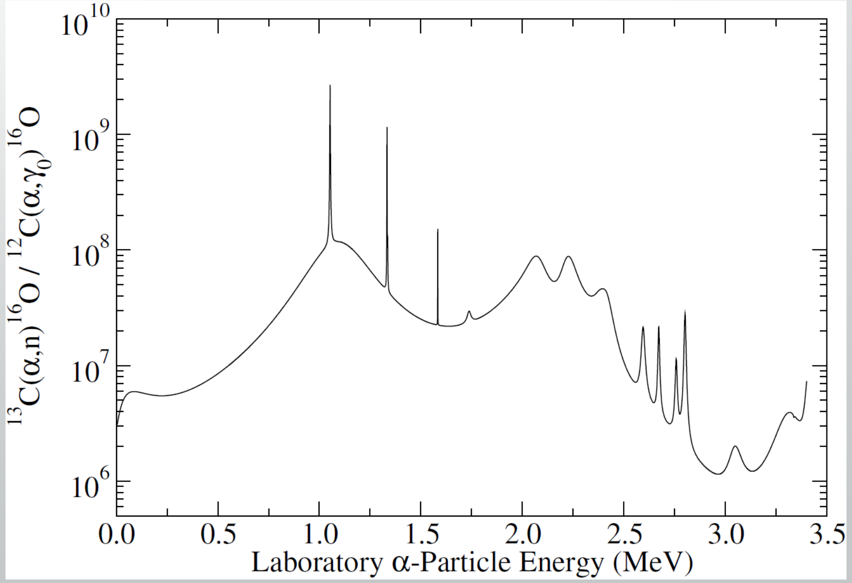

# Transfer reaction studies

- SubCoulomb measurements of Asymptotic Normalization Coefficients ($C_{\lambda c}$)

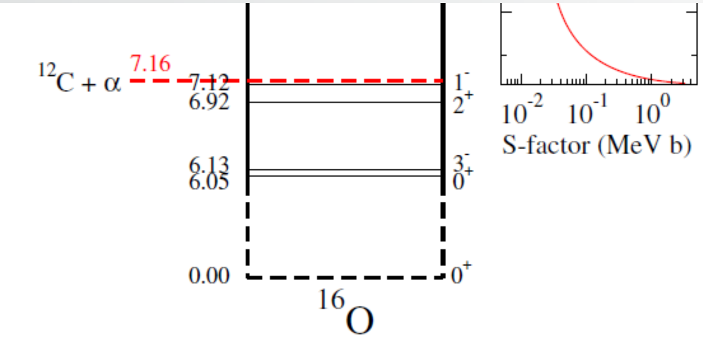

$$C_{\lambda c} = \frac{(2\mu_\alpha a_c)^{1/2}}{\hbar W_c(a_c)} \frac{\tilde{\gamma}_{\lambda c}}{[1 + \sum_{c'} \tilde{\gamma}^2_{\lambda c'} (dS_{c'}/dE)(\tilde{E}_\lambda)]^{1/2}},$$

## $^6$Li($^{12}$C,d)$^{16}$O or $^7$Li($^{12}$C,t)$^{16}$O

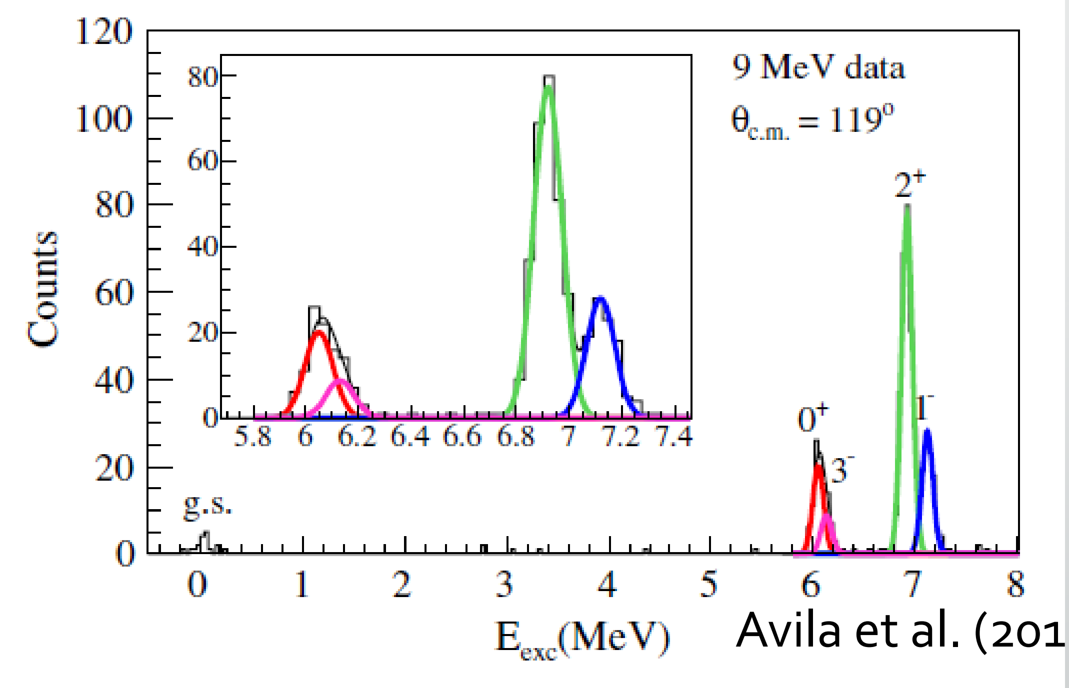

Avila et al. (2015)

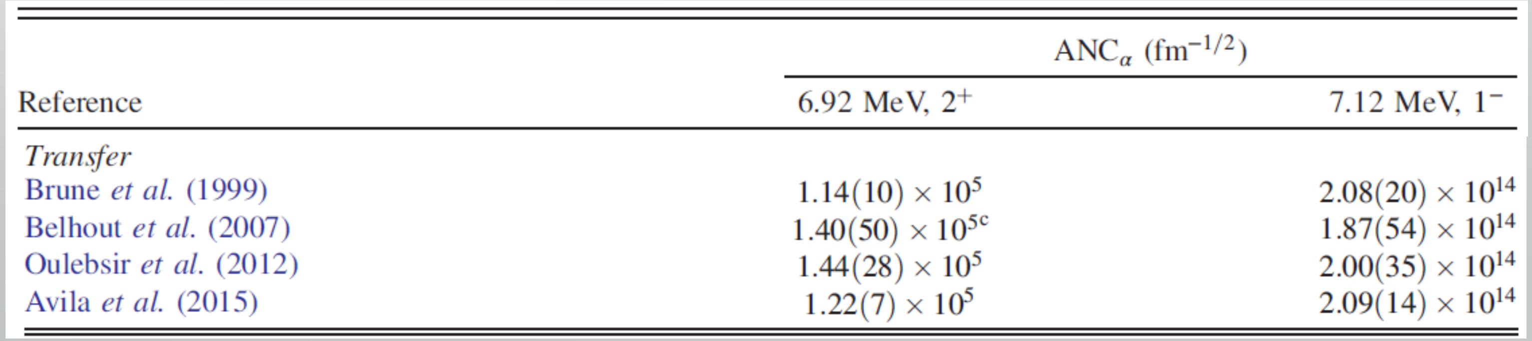

| Reference | ANC$_\alpha$ (fm$^{-1/2}$) | |
|---|---|---|
| | 6.92 MeV, $2^+$ | 7.12 MeV, $1^-$ |
| *Transfer* | | |
| Brune *et al.* (1999) | $1.14(10) \times 10^5$ | $2.08(20) \times 10^{14}$ |
| Belhout *et al.* (2007) | $1.40(50) \times 10^{5c}$ | $1.87(54) \times 10^{14}$ |
| Oulebsir *et al.* (2012) | $1.44(28) \times 10^5$ | $2.00(35) \times 10^{14}$ |
| Avila *et al.* (2015) | $1.22(7) \times 10^5$ | $2.09(14) \times 10^{14}$ |

# Other compound nucleus reactions

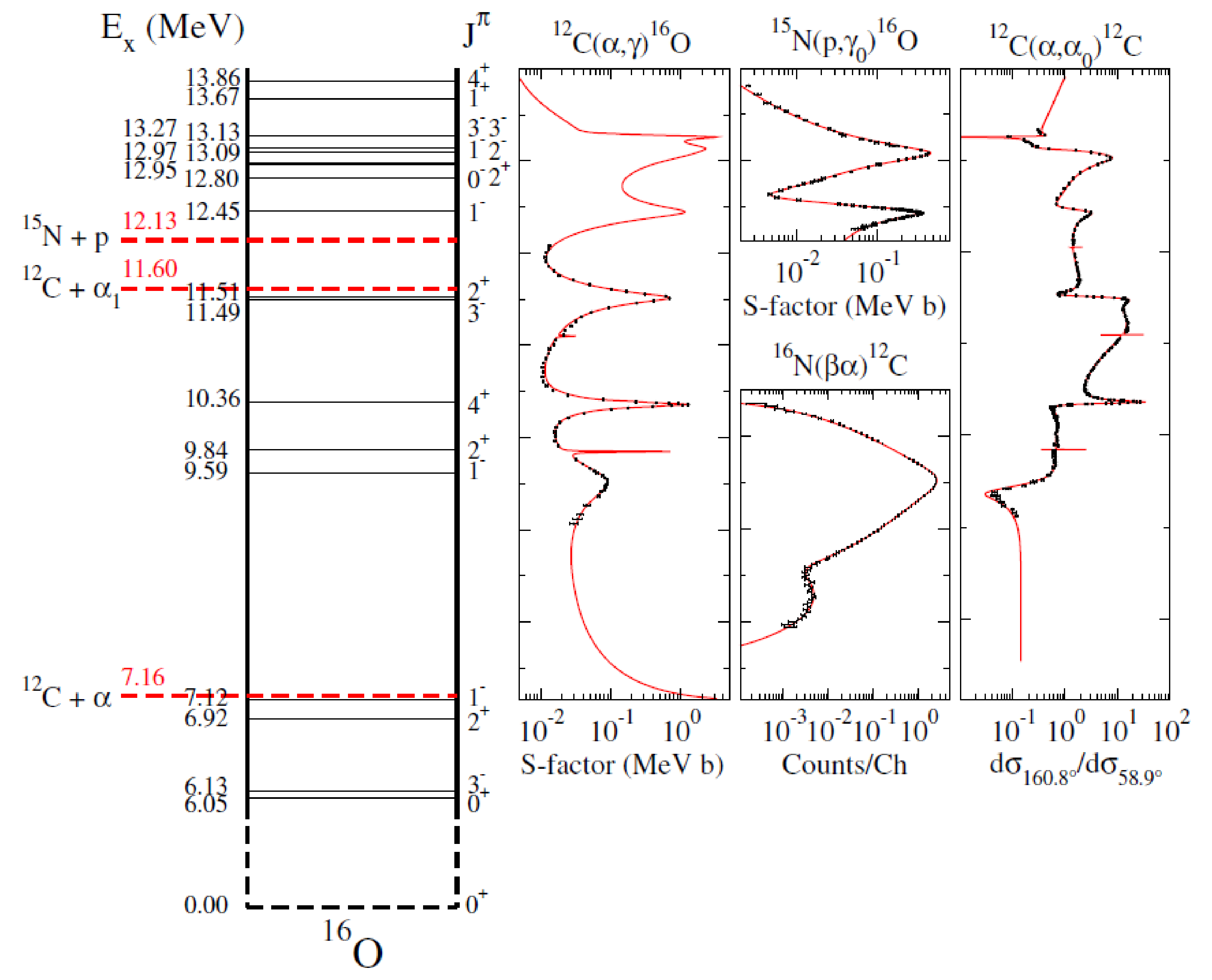

# Phenomenological R-matrix

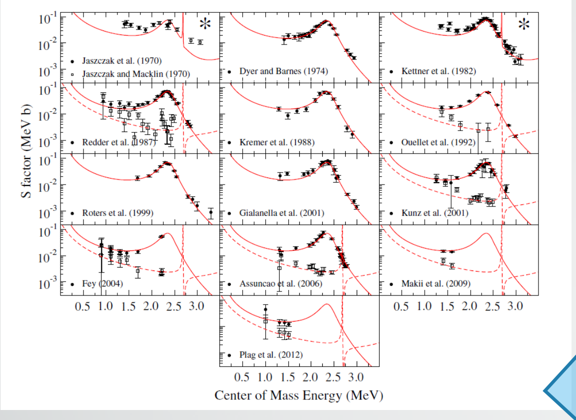

Low energy $^{12}$C(α,γ)$^{16}$O data

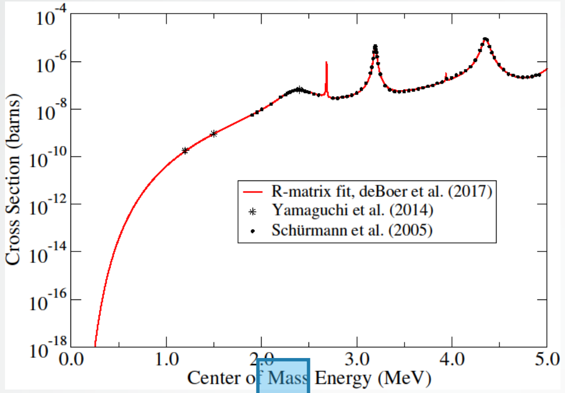

Total capture cross sections (recoils)

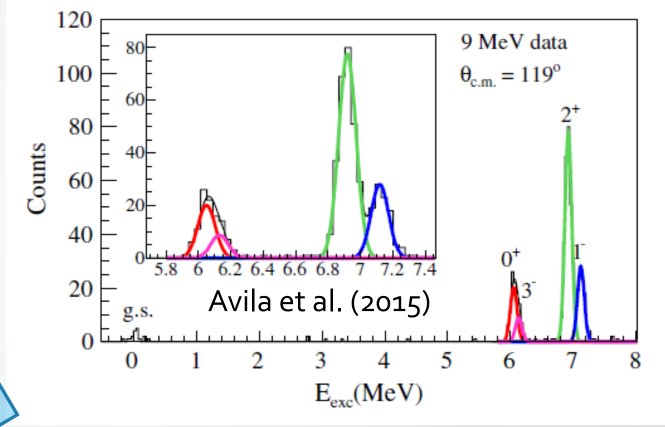

Bound state ANCs

$$R_{cc'} = \sum_{\lambda} \frac{\gamma_{\lambda c}\gamma_{\lambda c'}}{E_\lambda - E},$$

$^{16}$N(βα)$^{12}$C spectrum

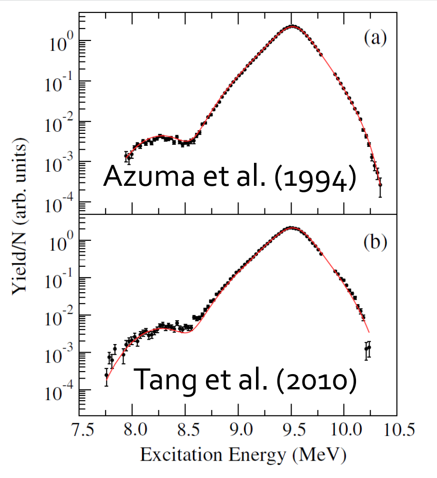

$^{12}$C(α,α)$^{12}$C data

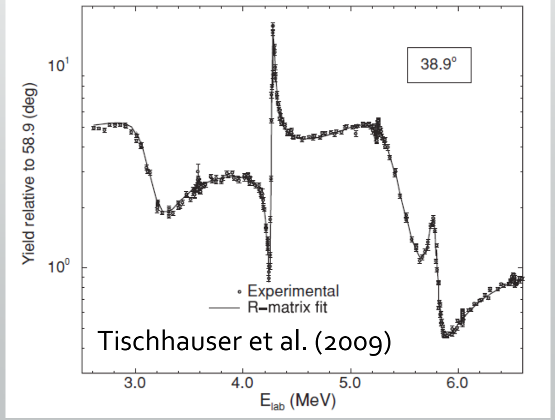

Multichannel R-matrix

$$\mathbf{U} = \boldsymbol{\rho}^{\frac{1}{2}}\mathbf{O}^{-1}(\mathbf{1}-\mathbf{R}\mathbf{L}_0)^{-1}(\mathbf{1}-\mathbf{R}\mathbf{L}_0^{*})\mathbf{I}\boldsymbol{\rho}^{-\frac{1}{2}}$$

$$T_{cc'} = e^{2i\omega_c}\delta_{cc'} - U_{cc'},$$

$$\sigma_{\alpha\alpha'} = \frac{\pi}{k_\alpha^2}\sum_{Jll'ss'} g_J \left|T^J_{cc'}\right|^2,$$

# Data inconsistencies

- “World data sets”
- Normalized here, but still show a lot of scatter
- Larger discrepancies in ground state E2 data
- However, more modern measurements have, usually, produced more consistent data

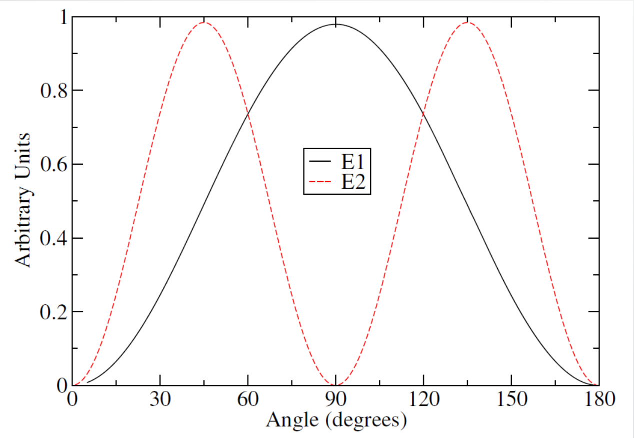

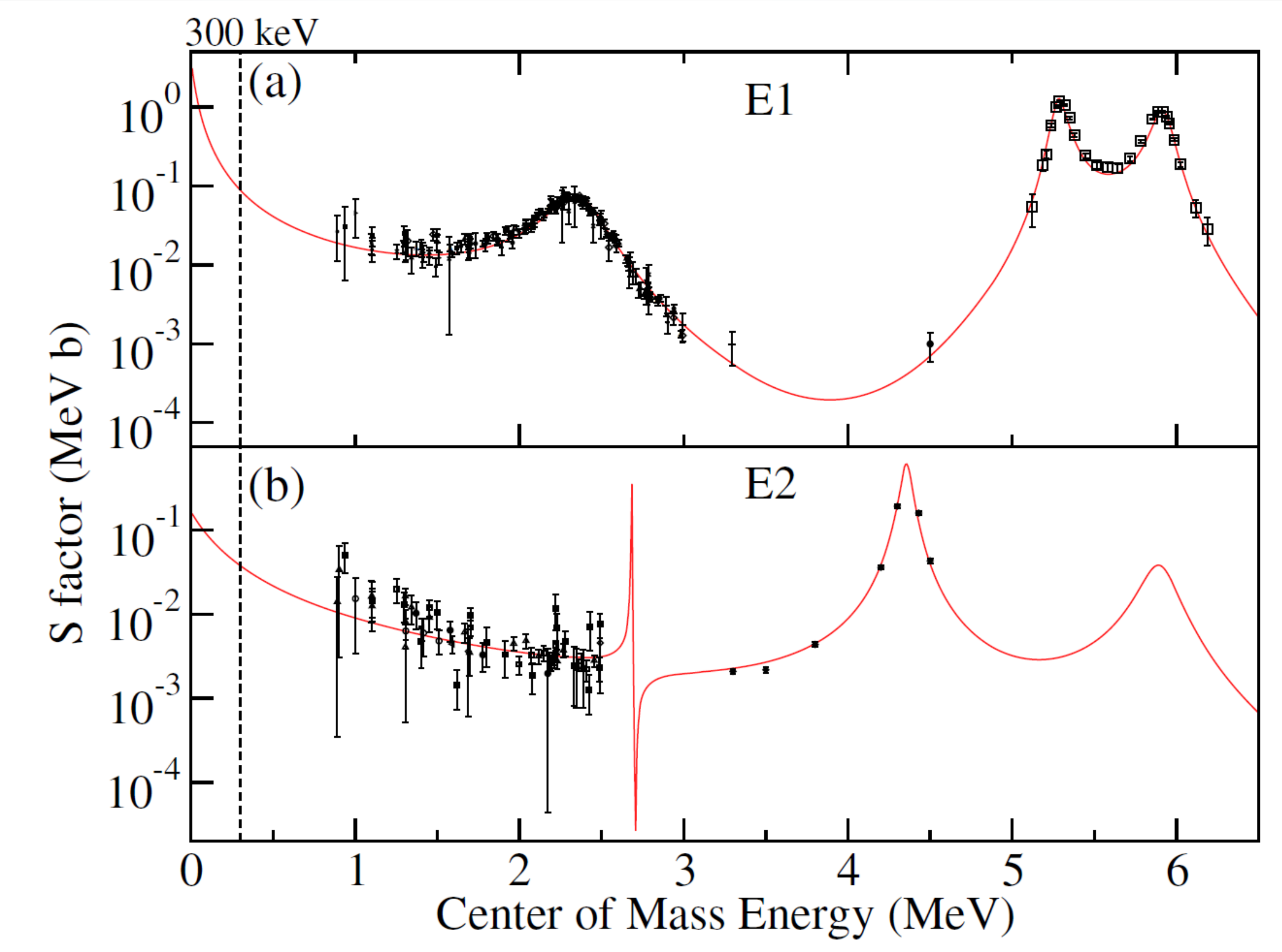

# Measurement Highlights: ERNA

- Schürmann *et al*. (2005, 2011)
- High precision total cross section measurement over a wide energy range
- Cascade transition measurements over a difficult range to access using standard methods
- Is extremely helpful in constraining background contributions in the R-matrix fit
- **New measurements under development at Caserta.**

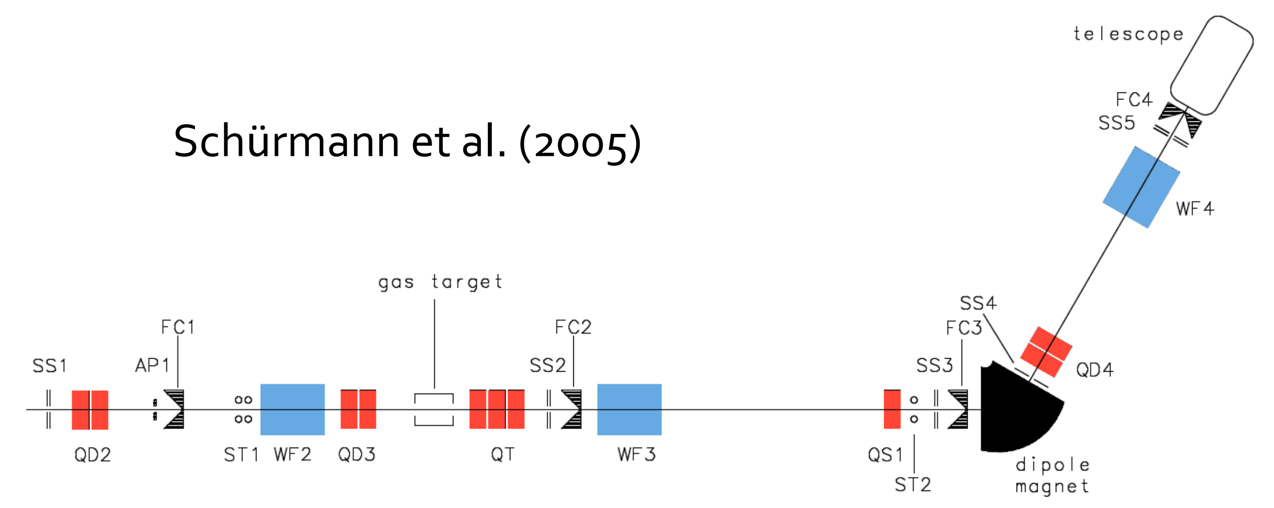
Schürmann et al. (2005)

Schürmann et al. (2005)

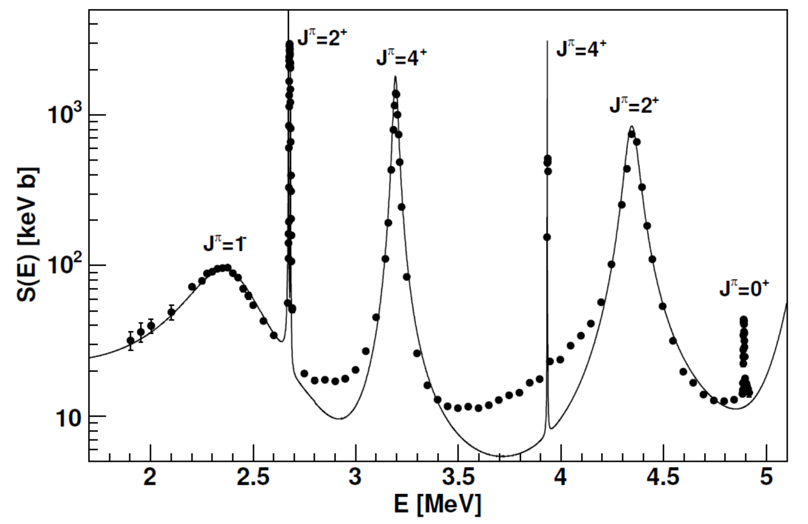

Schürmann et al. (2011)

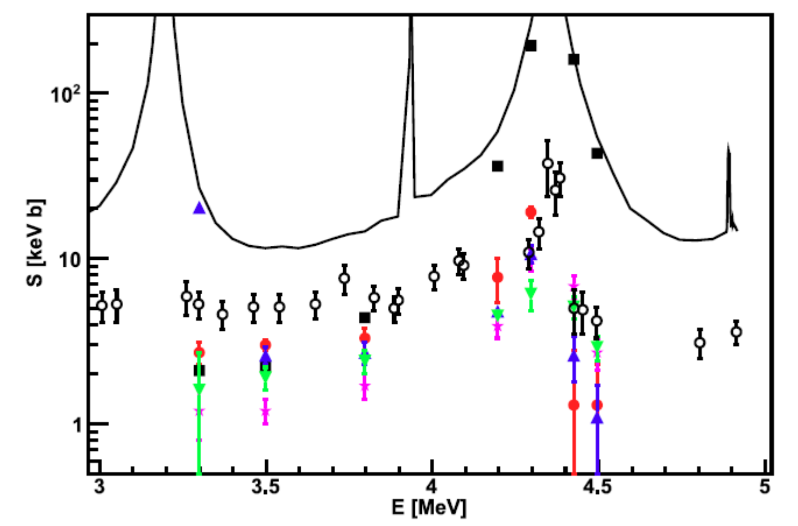

# Measurement Highlights: TAMU ANCs

- Avila et al. (2015)
- Built on the ground breaking **sub-Coulomb** transfer measurements by Brune et al. (1999)
- **$^{12}C(^{6}Li,d)^{16}O$**
- Improved measurements of the $2^+$ and $1^-$ ANCs, **first measurements of the $0^+$ and $3^-$ ANCs**
- Around 10% uncertainties achieved

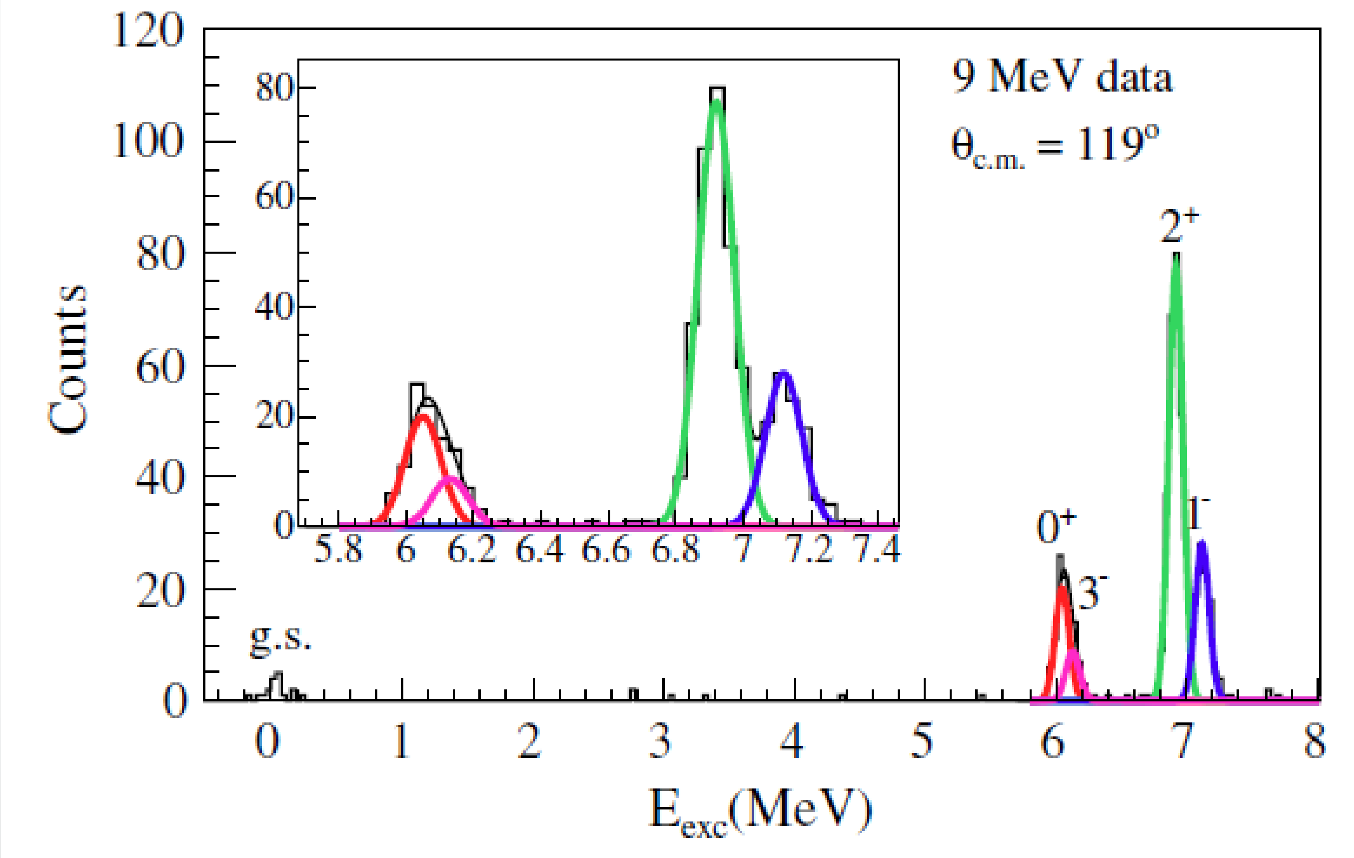

# Measurement Highlight: High Precision $^{12}C(\alpha,\gamma)^{16}O$ low energy measurements

- Plag et al. (2012)
- Used **time-of-flight** to separate out background from $(n,\gamma)$ reactions produced by neutrons from the $^{13}C(\alpha,n)^{16}O$ reaction
- $BaF_2$ array for **detailed angular distribution measurements**
- All angular distribution data is given, not just E1 and E2 data

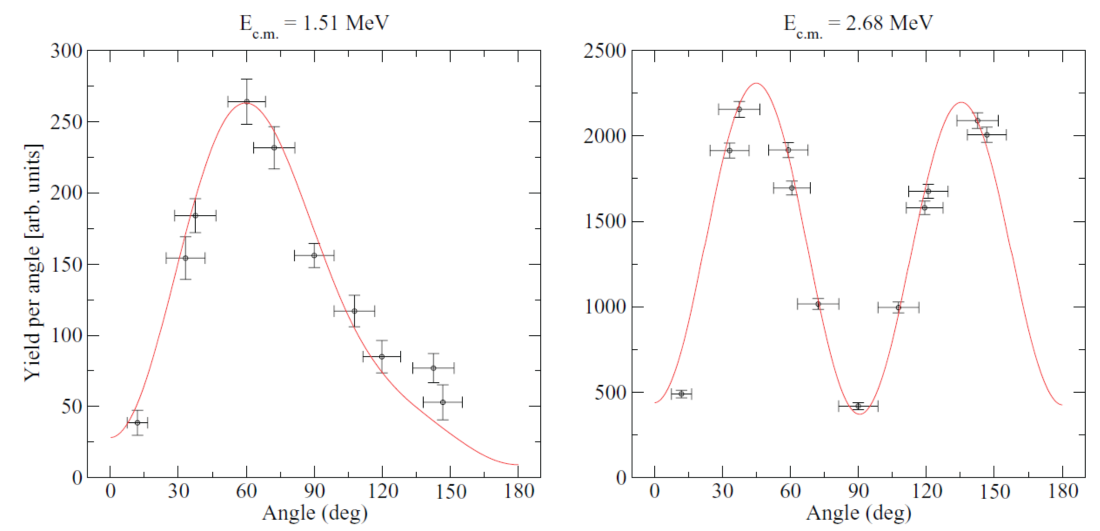

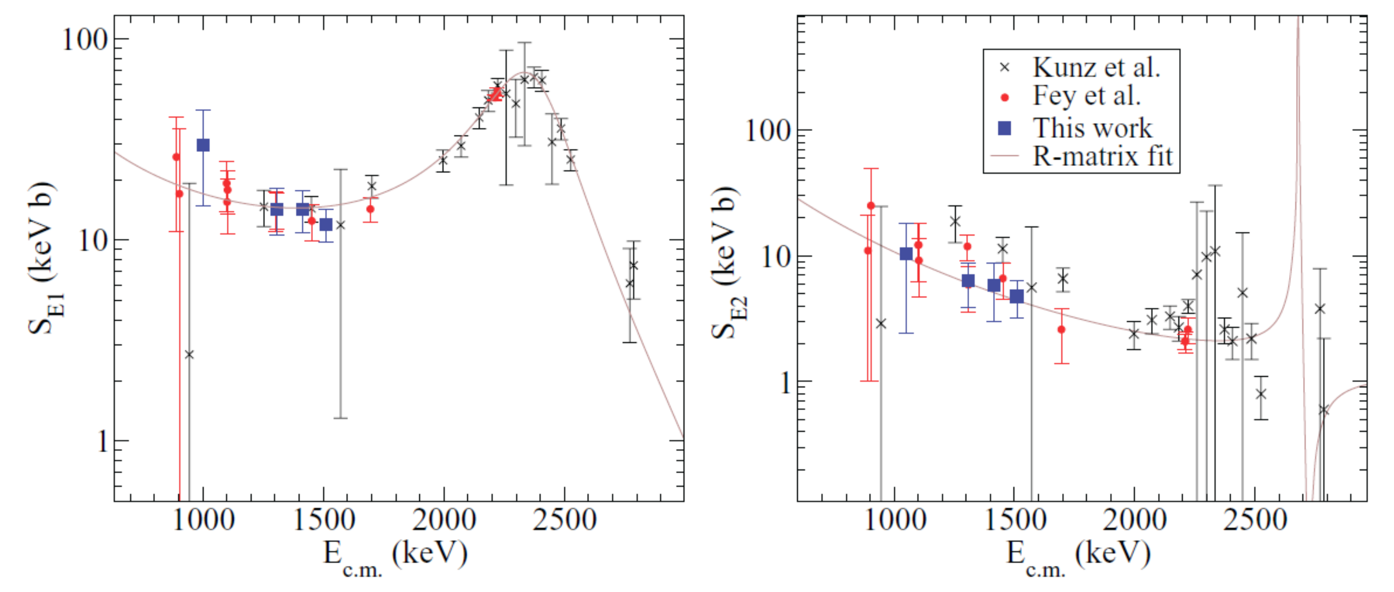

# Measurement Highlight : $^{16}O(\gamma,\alpha)^{12}C$

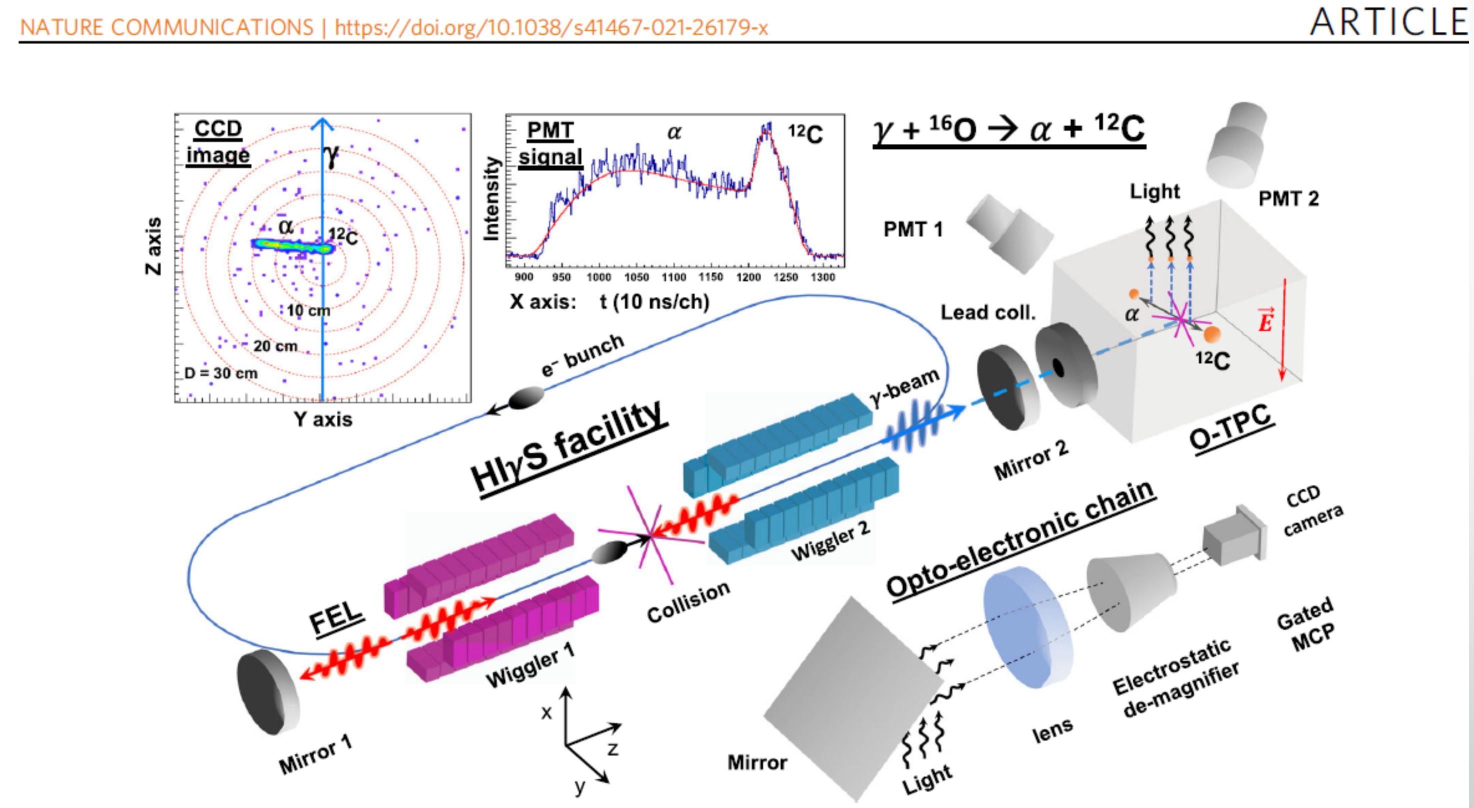

NATURE COMMUNICATIONS | https://doi.org/10.1038/s41467-021-26179-x ARTICLE

Long campaign (hundreds of hours) led by Moshe Gai

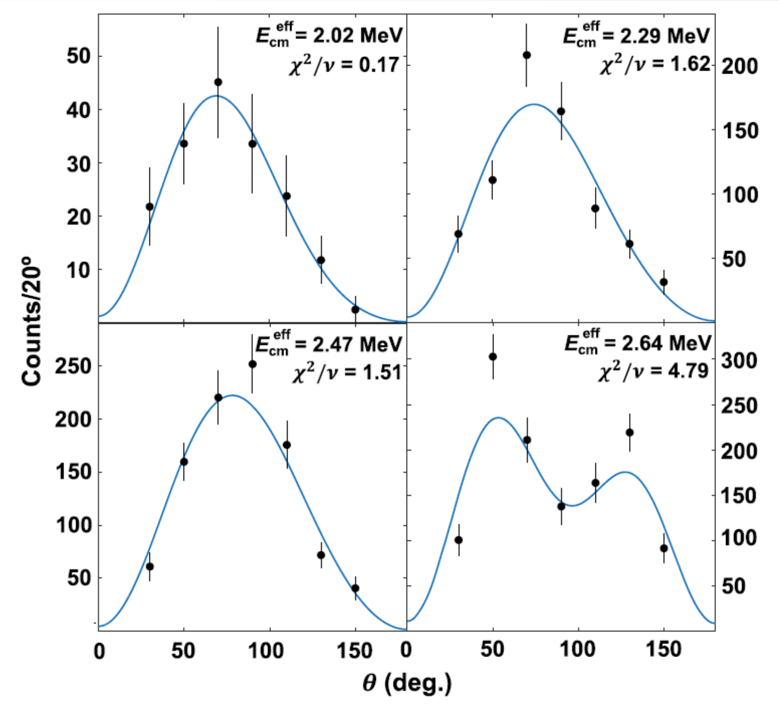

Smith *et al*. (2021)

# Measurement Highlight : Alternative transfer reactions

- Shen et al. (2019, 2020)
- **$^{12}C(^{11}B,^{7}Li)^{16}O$**
- Probing the model and reaction sensitivity of ANC determination
- $2^+$ ANC is re-measured in (2019)
- GS ANC is measured in (2020)

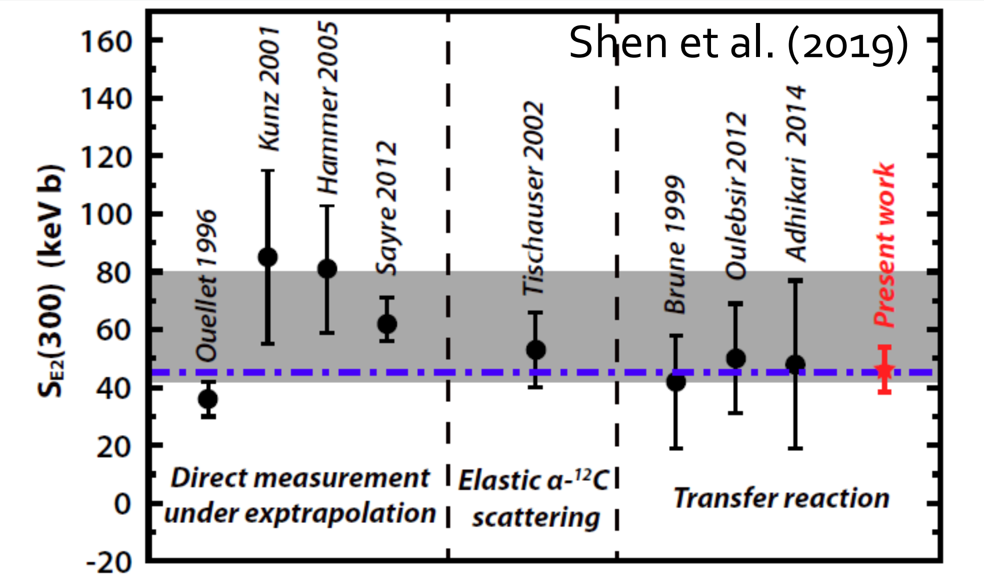
Shen et al. (2019)

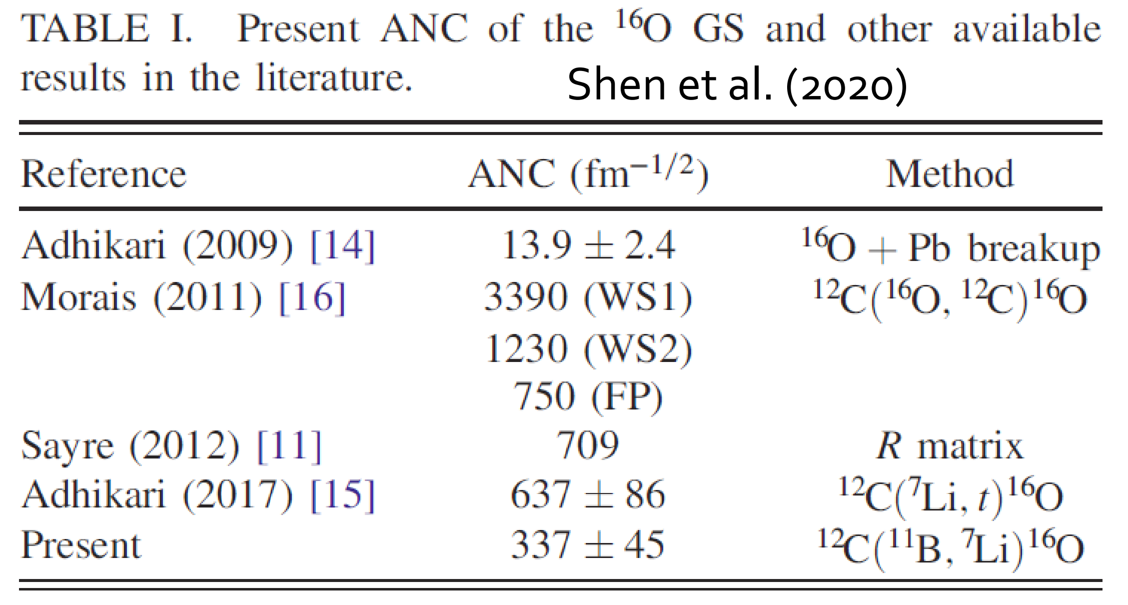
TABLE I. Present ANC of the $^{16}$O GS and other available results in the literature.

Shen et al. (2020)

| Reference | ANC ($fm^{-1/2}$) | Method |
|---|---|---|
| Adhikari (2009) [14] | 13.9 ± 2.4 | $^{16}O + Pb$ breakup |
| Morais (2011) [16] | 3390 (WS1)<br>1230 (WS2)<br>750 (FP) | $^{12}C(^{16}O, ^{12}C)^{16}O$ |
| Sayre (2012) [11] | 709 | *R* matrix |
| Adhikari (2017) [15] | 637 ± 86 | $^{12}C(^{7}Li, t)^{16}O$ |
| Present | 337 ± 45 | $^{12}C(^{11}B, ^{7}Li)^{16}O$ |

# On the horizon: $^{16}O(e,e'\alpha)^{12}C$

- MIT group
  - See Friščić et al. (2019)

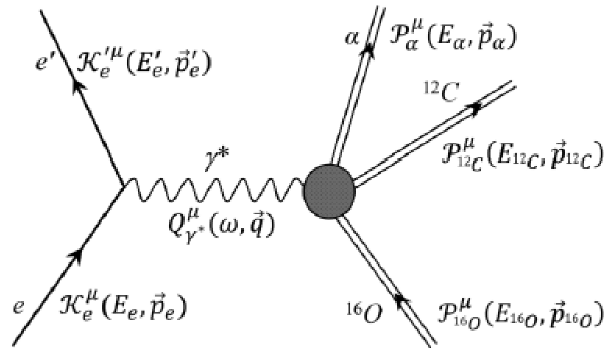

FIG. 3. First-order Feynman diagram for the electrodisintegration of $^{16}O$ involving one virtual photon $\gamma^*$ exchange to be compared with Fig. 2. Again, the kinematic variables here will be discussed in more detail in Sec. III.

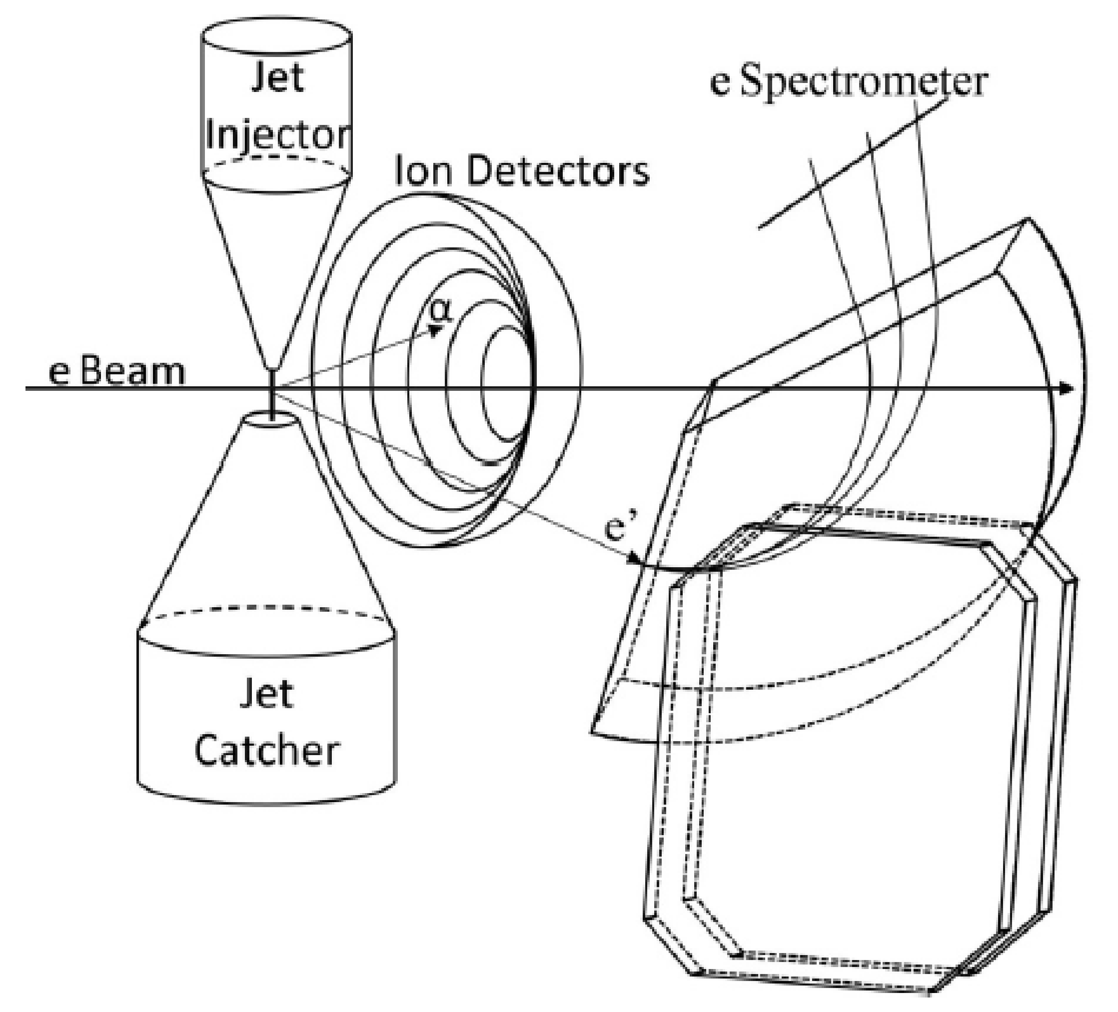

# On the horizon: $^{16}O(\gamma,\alpha)^{12}C$

- Jefferson Laboratory
- Ernst Rehm and Claudio Ugalde
- Bubble Chamber + Bremsstrahlung beam
- Previous tests at HIγS
- Not sure on current status?

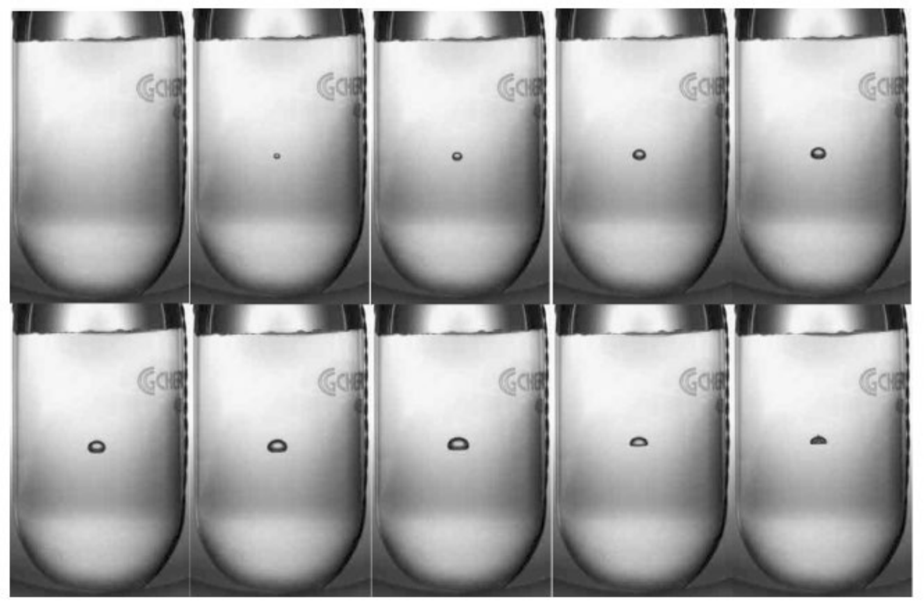

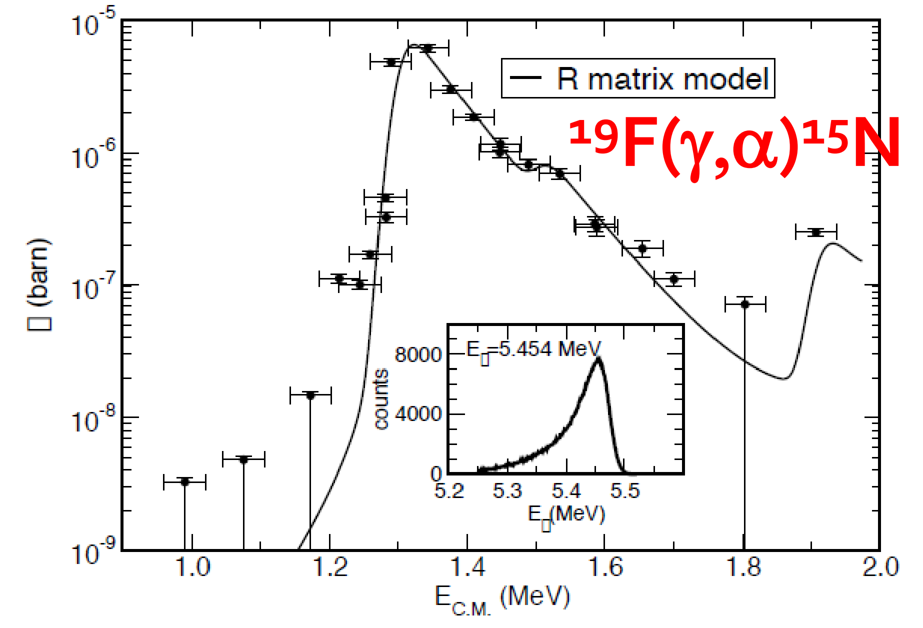

# On the horizon: Coulomb dissociation of $^{16}O$ on lead

- FAIR at GSI
  - Aims to get 10% uncertainty at 1 MeV
  - Will cover a wide energy range
  - Some measurements made, but still under analysis

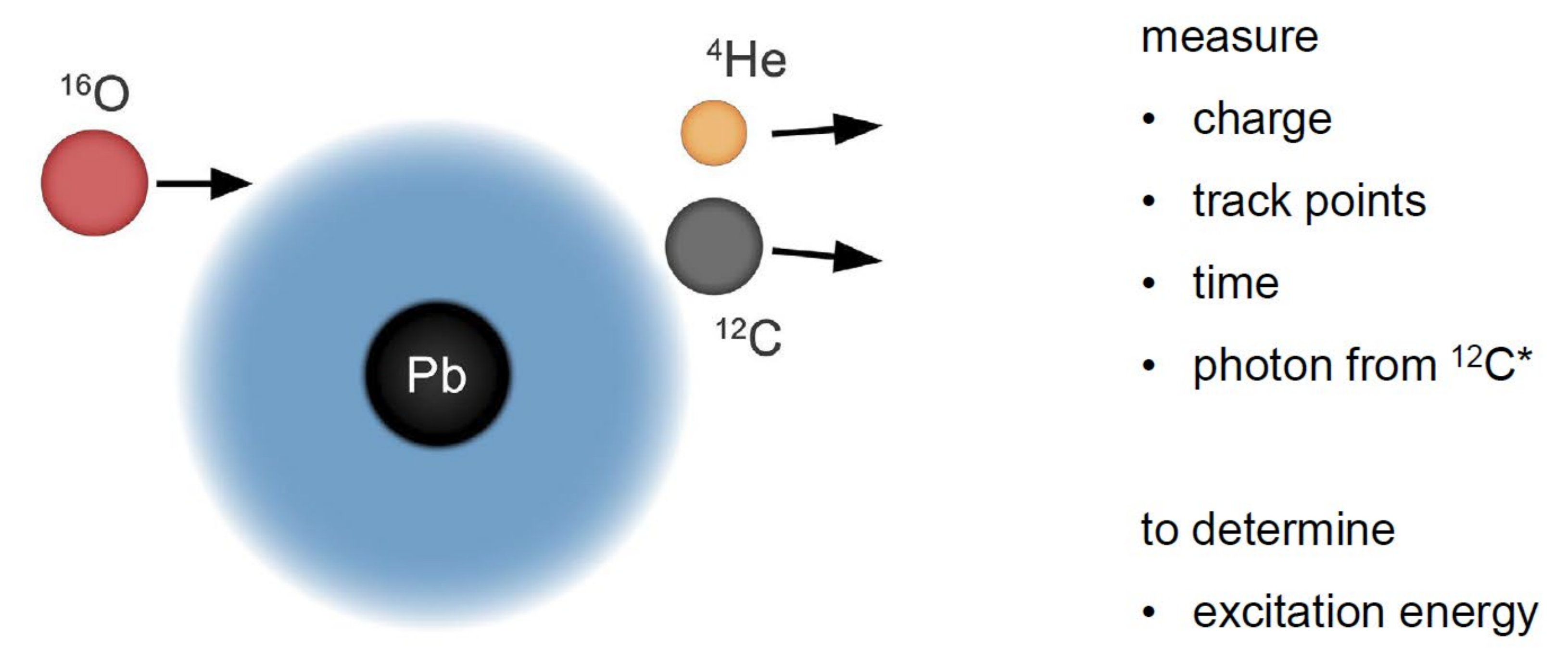

measure

- charge
- track points
- time
- photon from $^{12}C^*$

to determine

- excitation energy

Figure courtesy of Rene Reifarth

# On the Horizon: Felsenkeller planned Gas Jet Target based study of $^{12}C(\alpha,\gamma)^{16}O$

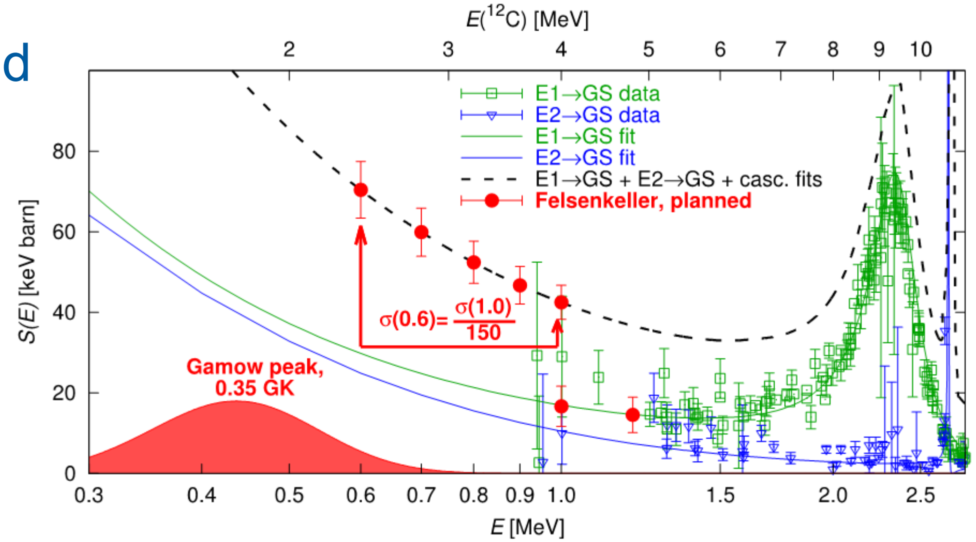

- $^{12}C(\alpha,\gamma)^{16}O$ potential for Felsenkeller with $^{12}C+$ beam, extended windowless $^{4}He$ gas target, $\gamma$-calorimeter, and $4\pi$ detector
- At Felsenkeller, planned to cover energy range from 0.6 – 2.0 MeV
- Gas target is complete, detector procurement is underway

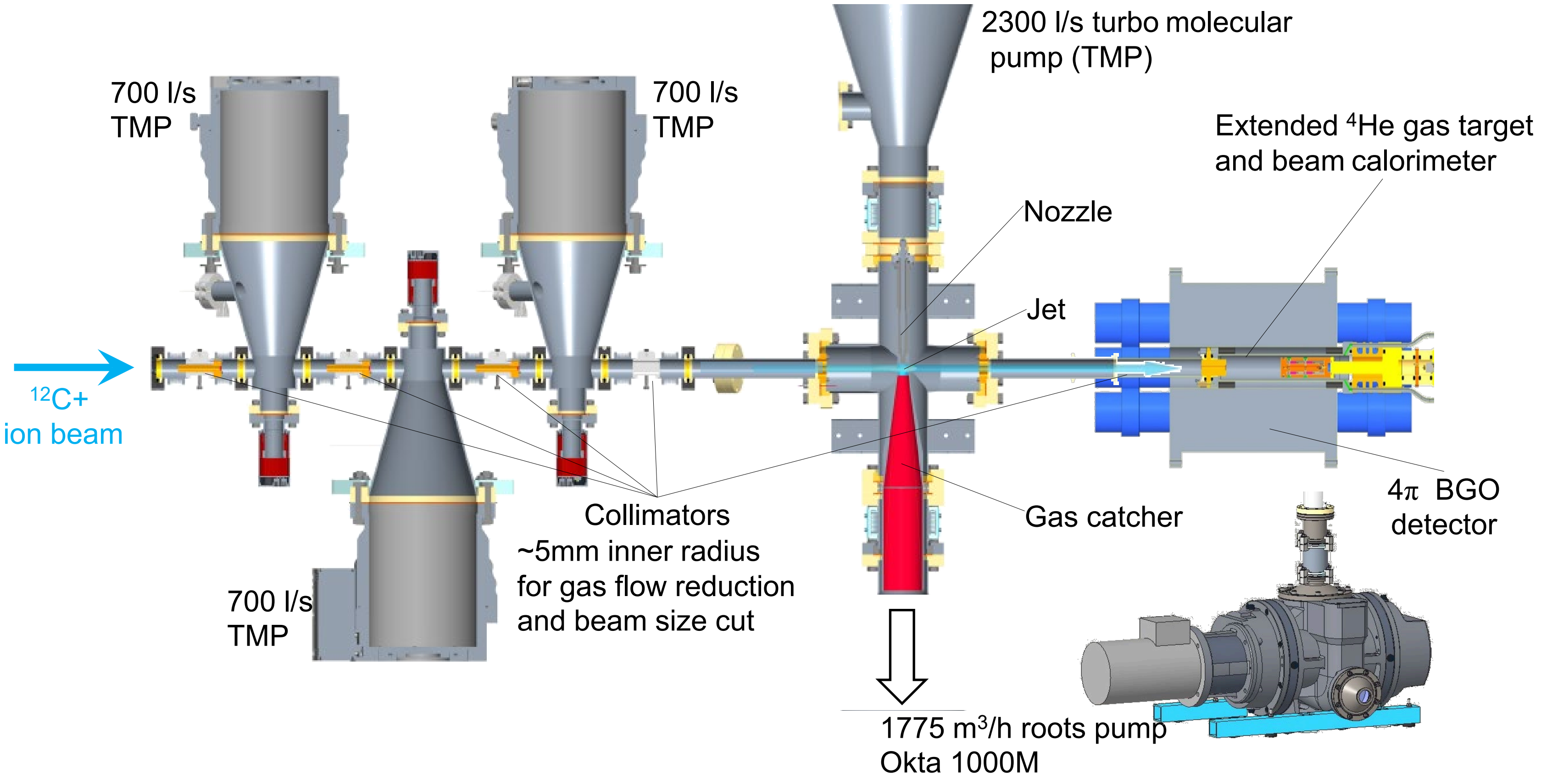

2300 l/s turbo molecular pump (TMP)

700 l/s TMP

700 l/s TMP

Extended $^{4}He$ gas target and beam calorimeter

Nozzle

Jet

$^{12}C+$ ion beam

4π BGO detector

Collimators ~5mm inner radius for gas flow reduction and beam size cut

Gas catcher

700 l/s TMP

1775 $m^3/h$ roots pump Okta 1000M

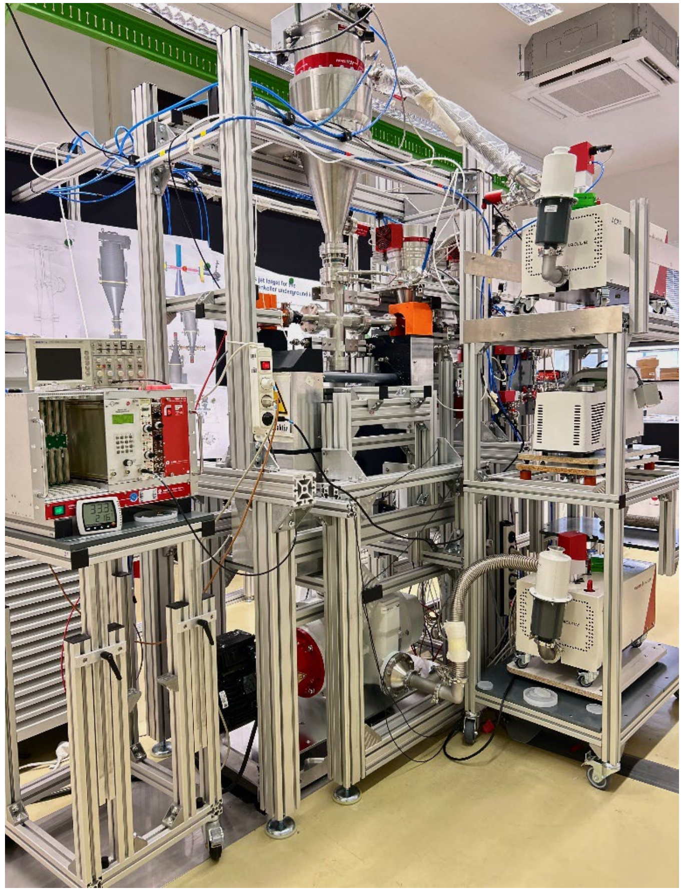

# On the Horizon: **Preliminary** Measurements from JUNA

Milliamp beam
TiC target

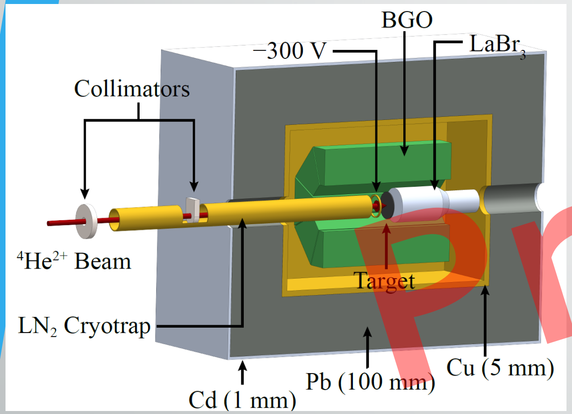

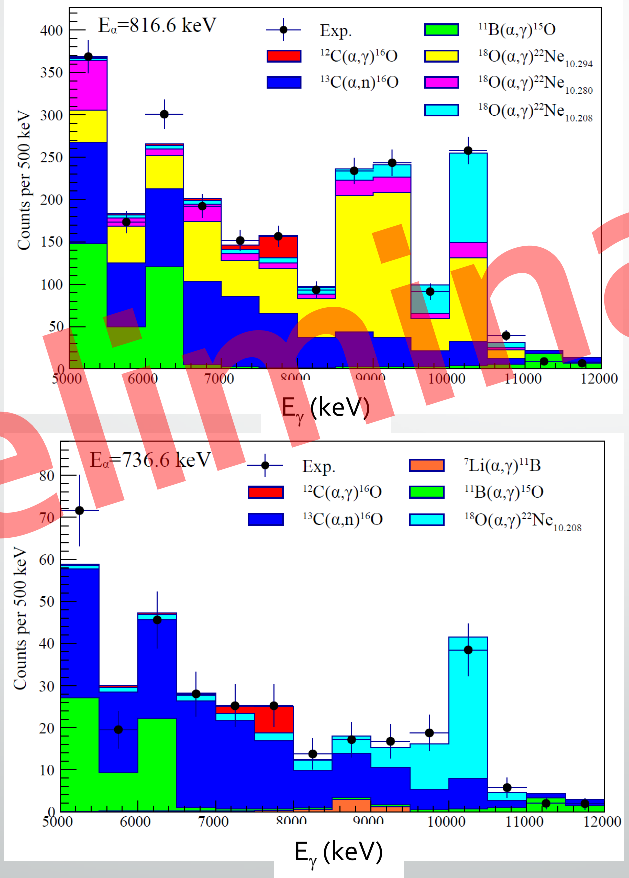

Submitted for publication, Y.P. Shen *et al.*

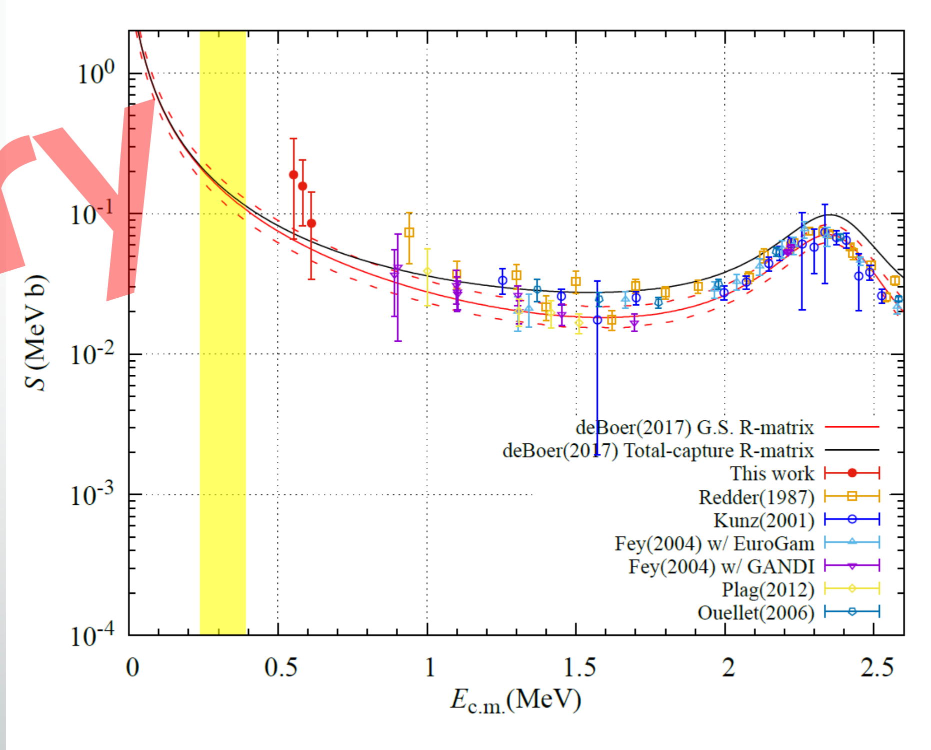

# Recent questions about $\alpha$ particle ANCs

- Revised $^6$Li ANC effects the ANCs of any ($^6$Li,d) type alpha transfer measurement
- In the case of $^{12}C(\alpha,\gamma)^{16}O$, it would imply **smaller** ANCs and therefore a smaller cross section by about 30%

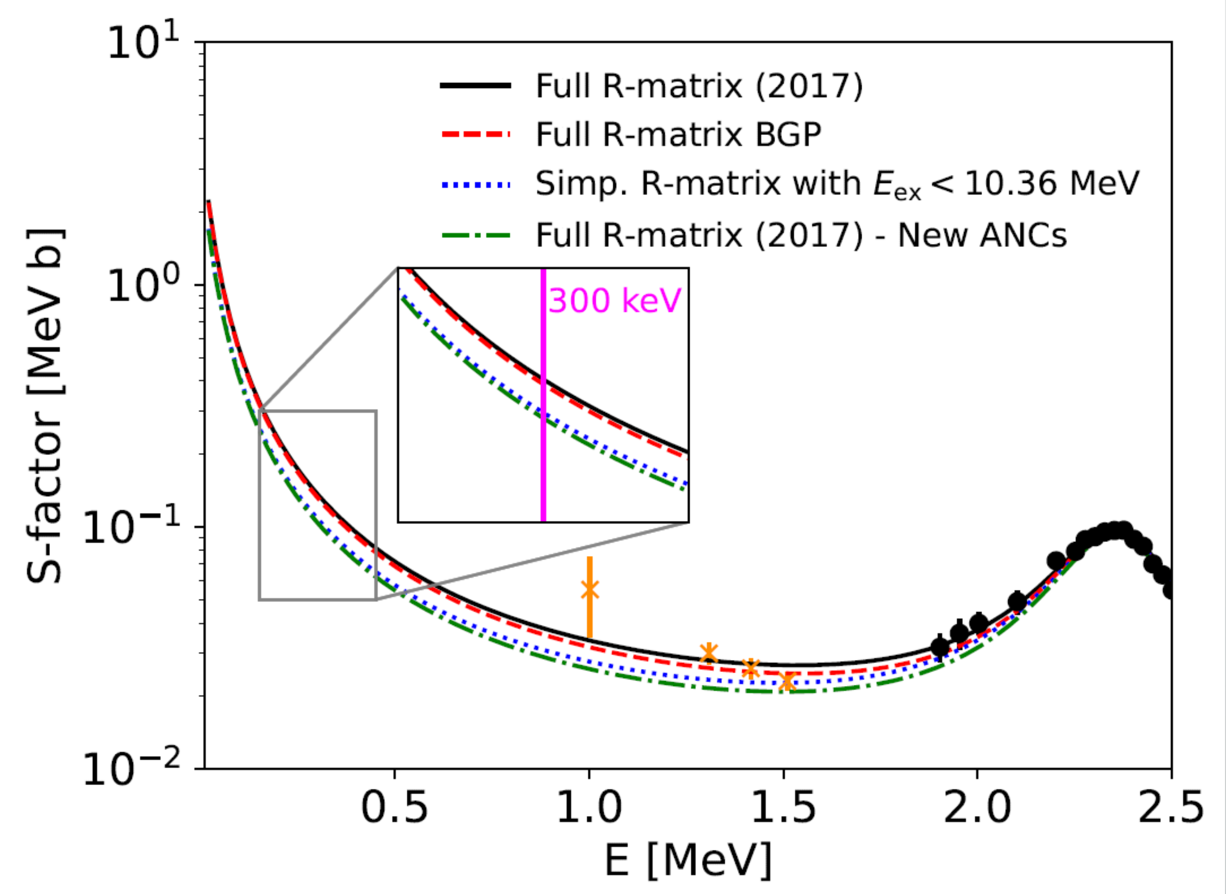

Hebborn *et al*. (arXiv, July 2023)

# Multiple GS and $2^+$ ANC solutions

Shen *et al.* (2020)

- $^{12}$C($^{11}$B,$^{7}$Li)$^{16}$O a transfer was used to measure the ground state ANC
- E2 external capture is small, but at very low energies its interference with the $2^+$ subthreshold state is substantial
- However, effect is lower in energy than we can measure directly
- Implies a **larger** $2^+$ ANC is needed

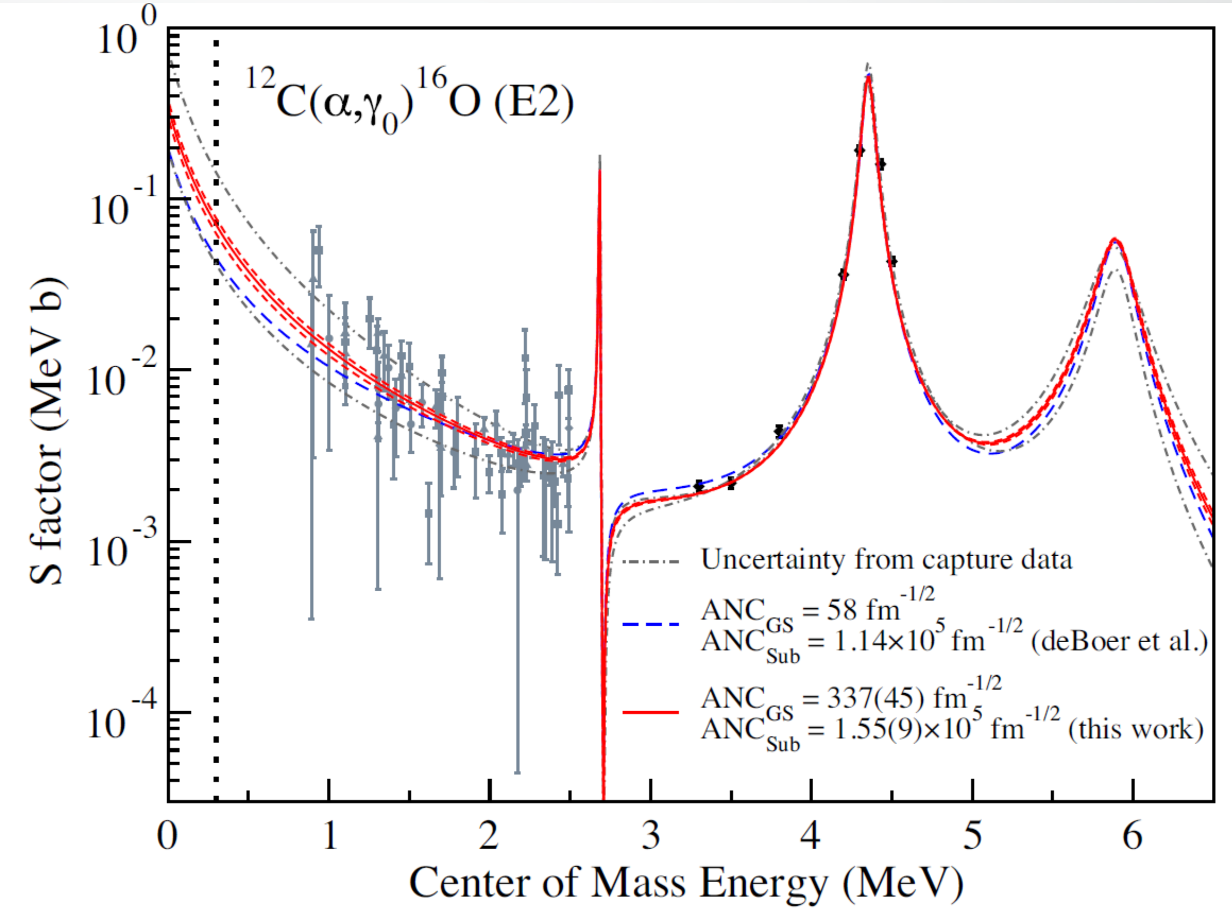

# Revised method of extracting ANCs from scattering phase shifts

- Blokhintsev *et al*. (2023), Mukhamedzhanov *et al*. (arXiv, 2024)
- Extraction of ANCs using Tisshauser *et al*. (2009) phase shifts
- Question about uncertainties
- **Larger** 2+ ANC (1.14 → 1.42)$10^5$ fm$^{-1/2}$

deBoer
et al. (2017)

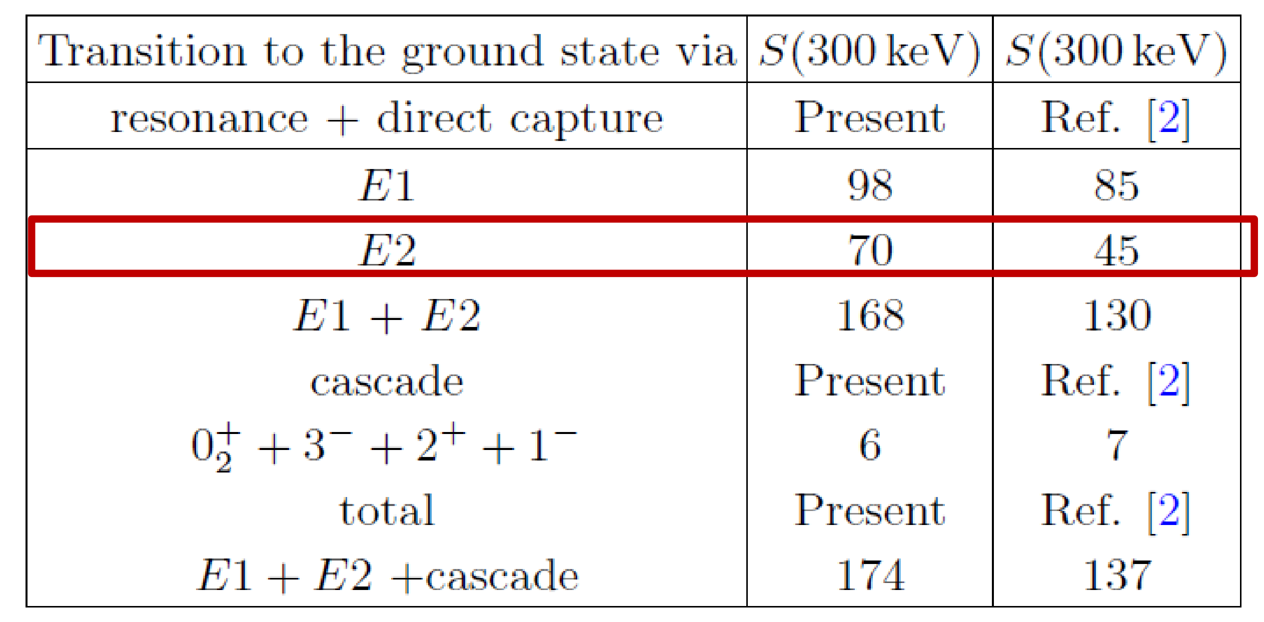

| Transition to the ground state via | $S(300\,\text{keV})$ | $S(300\,\text{keV})$ |
|---|---|---|
| resonance + direct capture | Present | Ref. [2] |
| $E1$ | 98 | 85 |
| $E2$ | 70 | 45 |
| $E1 + E2$ | 168 | 130 |
| cascade | Present | Ref. [2] |
| $0_2^+ + 3^- + 2^+ + 1^-$ | 6 | 7 |
| total | Present | Ref. [2] |
| $E1 + E2$ +cascade | 174 | 137 |

# Improvement in reaction rate tabulation!

- Reaction rates are tabulated over "standard" temperature grids.
- Astrophysics codes then interpolate the values given in tables
- Have to watch out for too few temperature steps!
- **Frank Timmes and Ebraheem Farag**

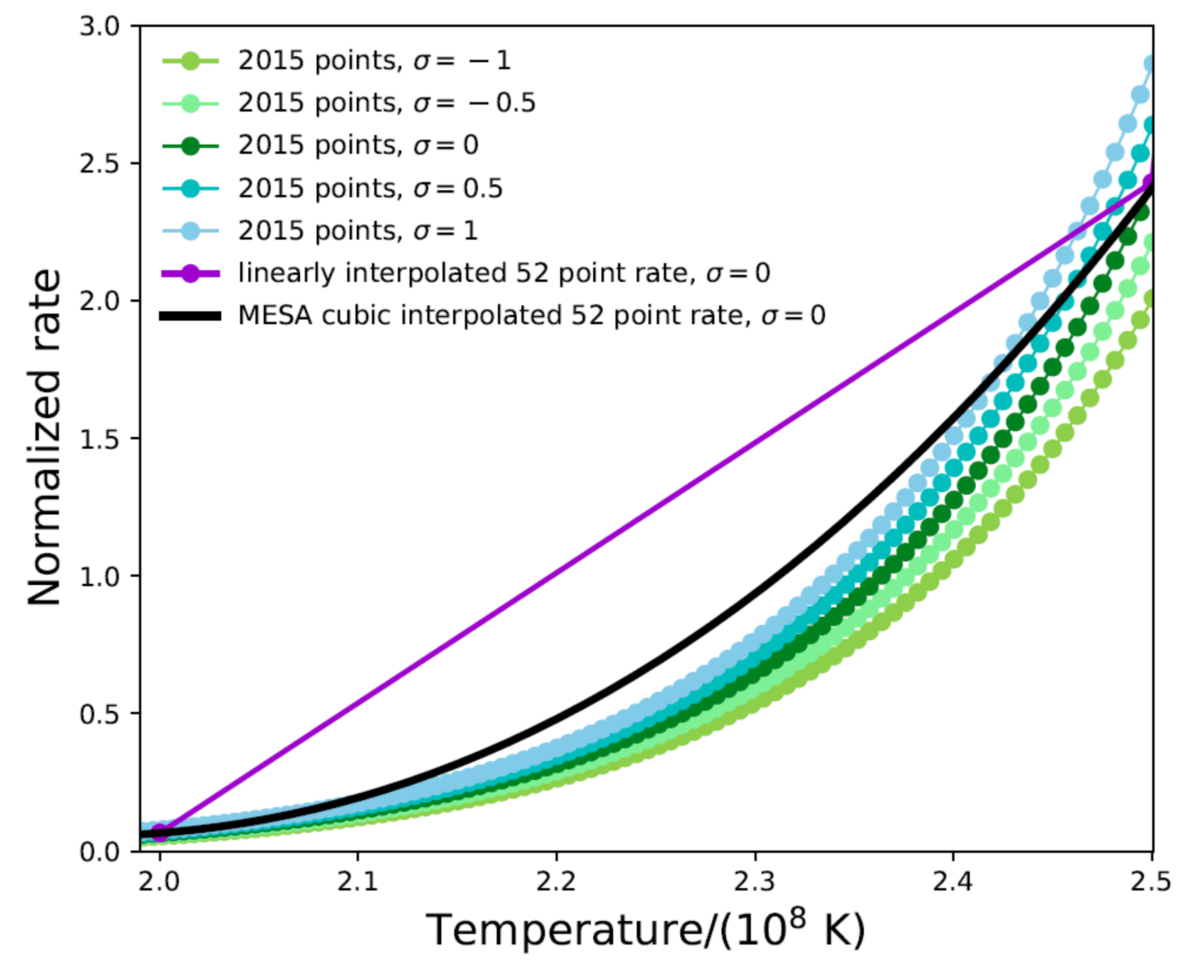

**MESA interpolation is off by more than 1σ for deBoer et al. (2017) tabulated rates!!!**

# The R-matrix fit ends up being a big multidimensional fit problem

- Fit parameters
  - Level energies
  - Level widths (or reduced width amplitudes)
  - Asymptotic Normalization Coefficients (or reduced width amplitudes)
  - Data normalization factors
- For the case described in the deBoer *et al.* (2017), there were 64 level parameters and over 100 data normalization fit parameters
- >10,000 experimental data points
- **Computationally challenging**

$$R_{cc'} = \sum_{\lambda} \frac{\gamma_{\lambda c}\gamma_{\lambda c'}}{E_{\lambda} - E},$$

# Improving uncertainty estimation for R-matrix fits

- A more general problem
- **Bayesian** methods provide a way to improve and gain more detailed information
- See de **Souza et al. (2020)** for an application to $^3$H(d,n)$^4$He
- Computationally intensive, but probably doable
- **Daniel Odell** at Ohio University has developed the Bayesian R-matrix Inference Code Kit (**BRICK**) for use with the **AZURE2** R-matrix code

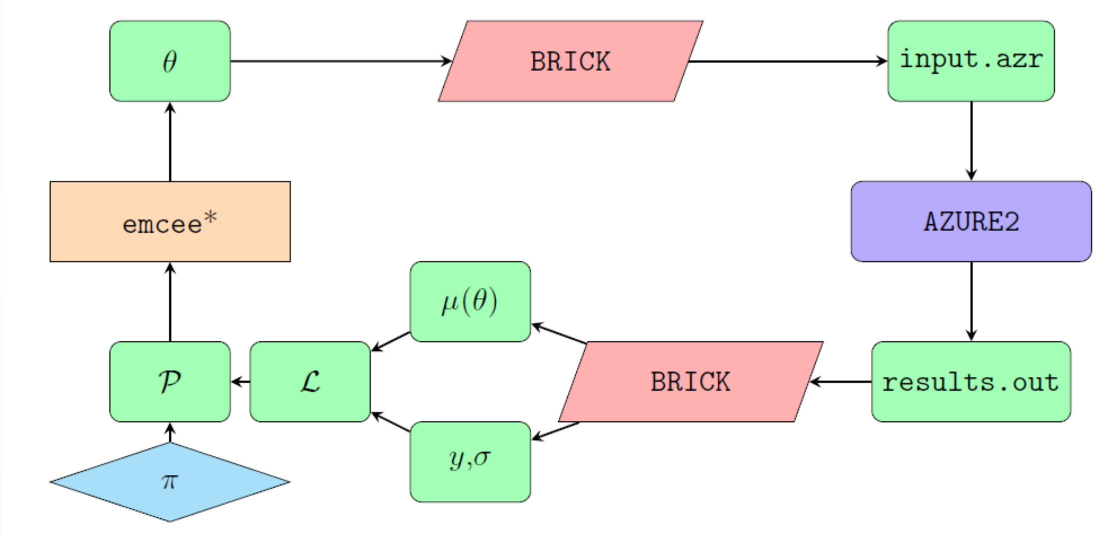

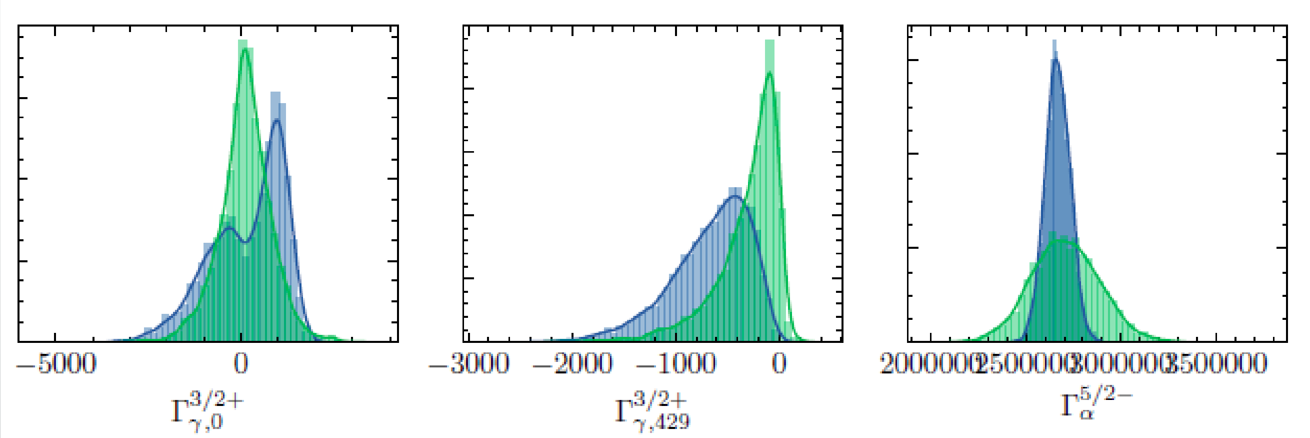

Figures courtesy of Daniel Odell

# Summary

- Improvements in the uncertainty of the low energy S-factor are hampered by **inconsistent data**
  - **Newer data are much more consistent!** We're on the right track, but measurements are very challenging
  - **Ground state E2 data is in the worst shape**, because you usually need to measure a more complete angular distribution to obtain it
  - **ERNA recoil separator measurements provided a LOT more constraint for the R-matrix fit because they covered a wide energy range.** More of these type measurements would be very useful!
- Make new measurements using new techniques (reduce systematic uncertainties)
  - $^{16}O(\gamma,\alpha)^{12}C$ (HI$\gamma$S, Jefferson Lab, ELI-NP)
  - $^{16}O(e,e'\alpha)^{12}C$
  - Additional types of transfer measurements
  - Improved traditional measurements, but in low background environments with very high beam intensities (reduce statistical / outlier uncertainties)
    - **JUNA, LUNA, Dresden**
- Include more detailed experimental uncertainties
    - Energy uncertainty, experimental resolution
    - **Bayesian** uncertainty estimation
    - Improved computational resources

# Questions?

My 2017 estimate of S(300 keV):

140 ± 21 (MC) +18/-11 (model)

But see Shen *et al*. (2020)

Assumes ANC uncertainties are accurate

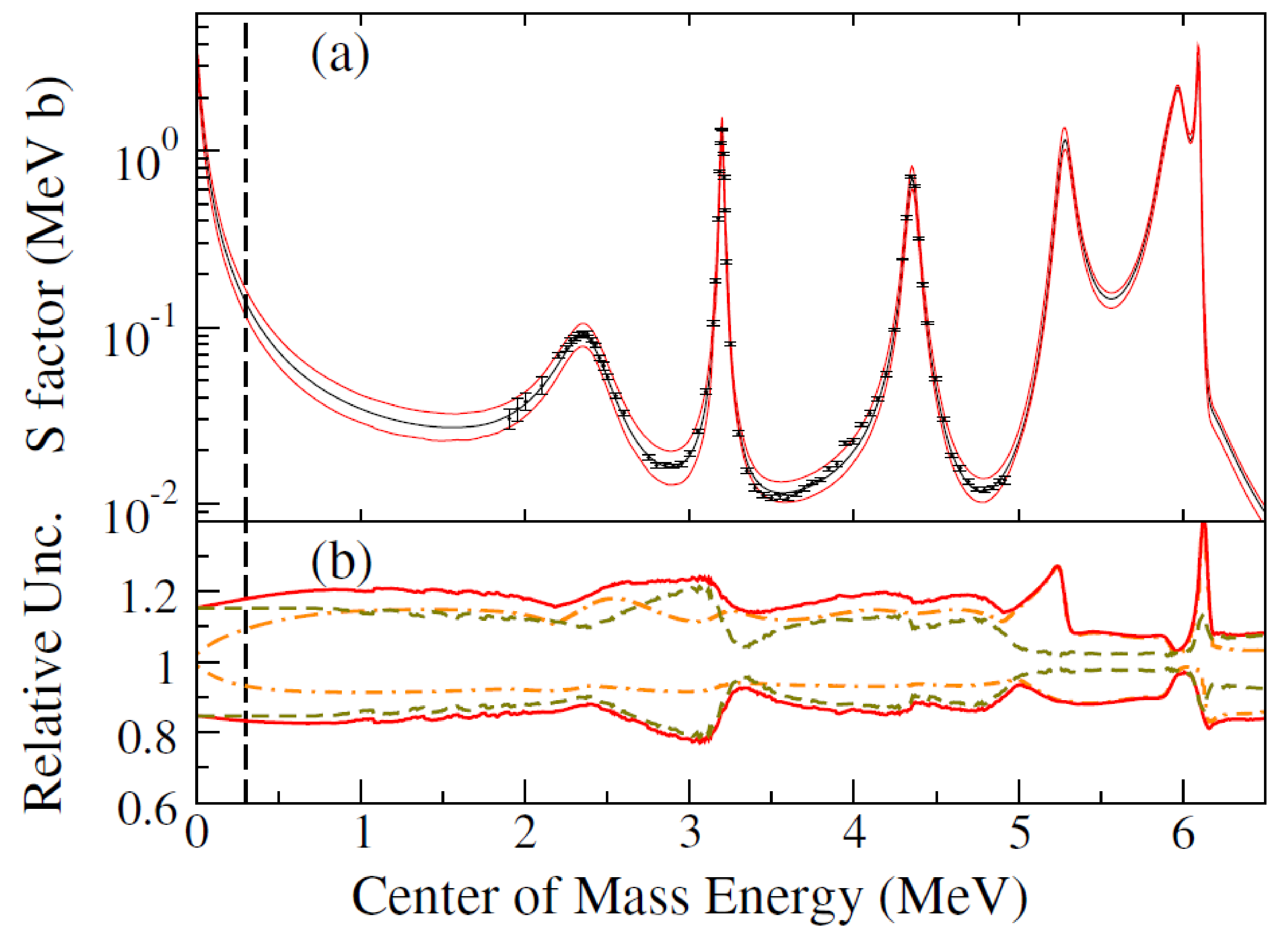

# Strategy in 2017 (and earlier)

- Use $\chi^2$ minimization to find a best description of the data within the R-matrix framework (used MINUIT2)

$$R_{ij} = \frac{f(x_{i,j}) - n_i y_{i,j}}{n_i \sigma_{i,j}}$$

$$\chi^2 = \sum_i \left( \frac{\sum_j R_{ij}^2}{N_i - \nu} \right) + \frac{(n_i - 1)^2}{n_i^2 \sigma_{\mathrm{syst},i}^2}$$

Additional data normalization fit parameter, with common systematic uncertainty. Also fitting to *reduced* $\chi^2$.

$$\chi^2 = \sum_i \left( \frac{\sum_j R_{ij}^2}{N_i} \right) + \frac{(n_i - 1)^2}{n_i^2 \sigma_{\mathrm{syst},i}^2} + \sum_k \frac{(P_{\mathrm{fit},k} - P_{\mathrm{exp},k})^2}{\sigma_{\mathrm{exp},k}^2}$$

Add additional terms for subthreshold ANC to include uncertainty constraints from transfer reactions.

$$L = \sum_j \log \left[ \frac{1 - e^{-R_{ij}^2/2}}{R_{ij}^2} \right]$$

Sivia and Skilling (2006)

Used a broader distribution function for data point uncertainties (larger tails than a Gaussian)

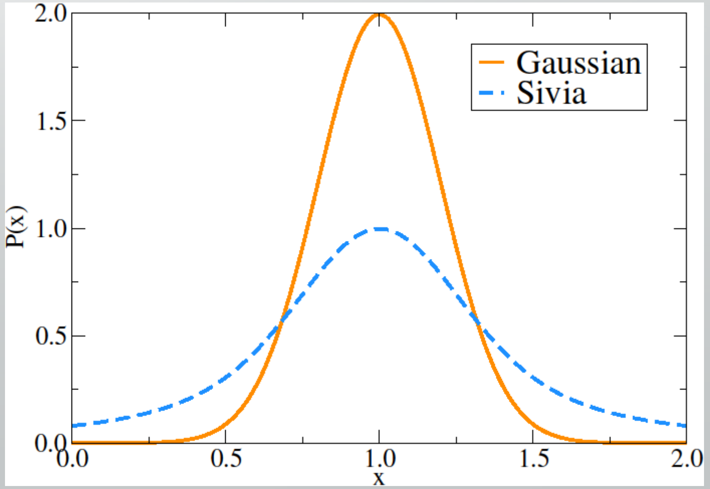

**Kind of a Frequentist / Bayesian hybrid method**

# R-matrix framework

$$R_{cc'} = \sum_{\lambda} \frac{\gamma_{\lambda c}\gamma_{\lambda c'}}{E_{\lambda} - E},$$

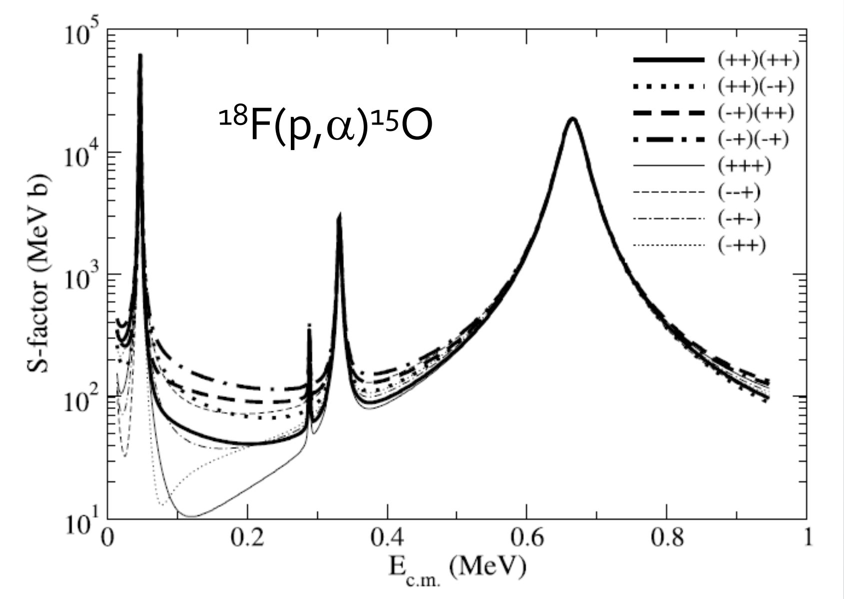

Bardayan et al. (2015)

$$\mathbf{U} = \rho^{\frac{1}{2}}\mathbf{O}^{-1}(\mathbf{1} - \mathbf{R}\mathbf{L}_0)^{-1}(\mathbf{1} - \mathbf{R}\mathbf{L}_0^*)\mathbf{I}\rho^{-\frac{1}{2}}$$

$$T_{cc'} = e^{2i\omega_c}\delta_{cc'} - U_{cc'},$$

$$\sigma_{\alpha\alpha'} = \frac{\pi}{k_{\alpha}^2} \sum_{Jll'ss'} g_J \left| T_{cc'}^J \right|^2,$$

# Simple Monte Carlo

- Created thousands of "synthetic" data sets by assuming that the error bars on the data represented an underlying Gaussian (probably should have used lognormal) Probability Density Function.
- Refit
- Histogrammed S-factor calculated at many energies to get uncertainty.
- Calculated many different variations on assumptions about the *R*-matrix fit and included those as well.
- Even more computationally expensive

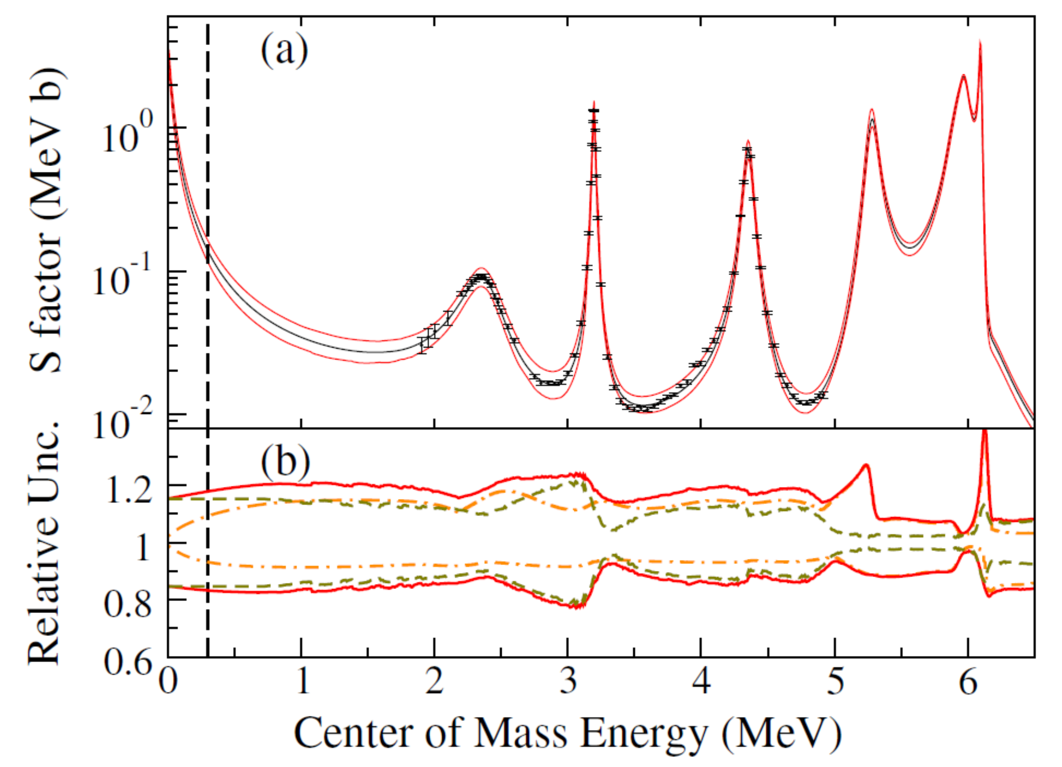

Monte Carlo of experimental data

**Model uncertainties**

# Model assumptions

- External capture contribution for GS?
  - Often neglected completely
  - May play a significant role in the E2 cross section (given recent improvements in the uncertainty of this cross section)
- Inconsistent measurements of the ground state $\alpha$-particle ANC in $^{16}$O
- Additional measurements needed!

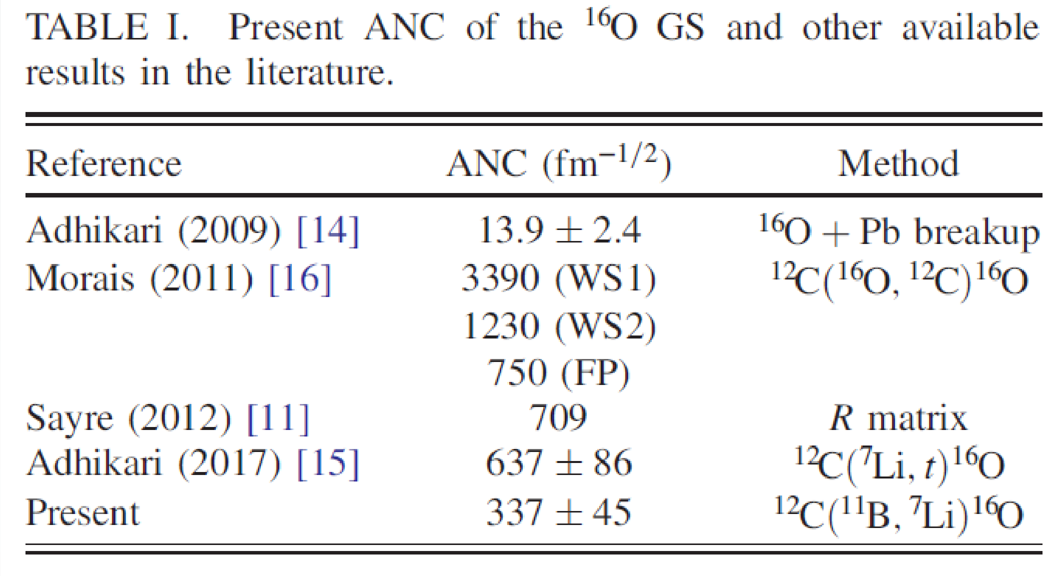

TABLE I. Present ANC of the $^{16}$O GS and other available results in the literature.

| Reference | ANC ($\mathrm{fm}^{-1/2}$) | Method |
|---|---|---|
| Adhikari (2009) [14] | $13.9 \pm 2.4$ | $^{16}$O + Pb breakup |
| Morais (2011) [16] | 3390 (WS1) | $^{12}\mathrm{C}(^{16}\mathrm{O}, ^{12}\mathrm{C})^{16}\mathrm{O}$ |
| | 1230 (WS2) | |
| | 750 (FP) | |
| Sayre (2012) [11] | 709 | *R* matrix |
| Adhikari (2017) [15] | $637 \pm 86$ | $^{12}\mathrm{C}(^{7}\mathrm{Li}, t)^{16}\mathrm{O}$ |
| Present | $337 \pm 45$ | $^{12}\mathrm{C}(^{11}\mathrm{B}, ^{7}\mathrm{Li})^{16}\mathrm{O}$ |

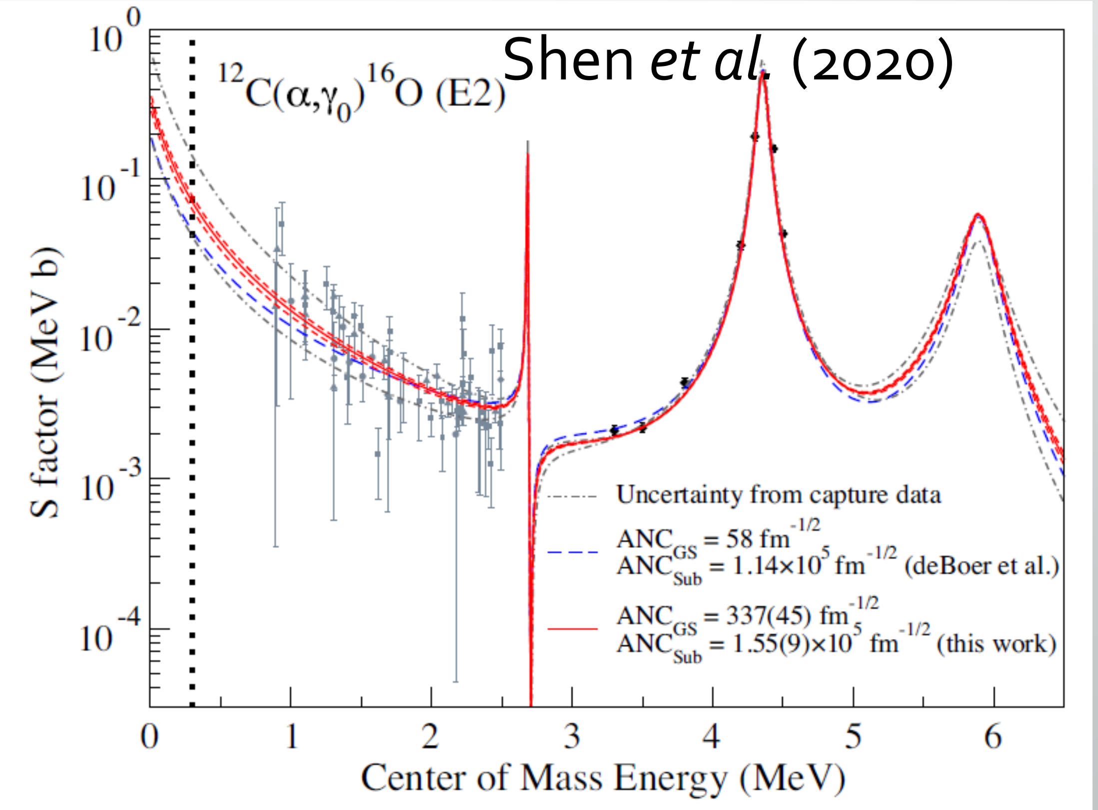

Shen *et al.* (2020)

# Background contributions

- General issue in the R-matrix framework

$$R_{cc'} = \sum_{\lambda} \frac{\gamma_{\lambda c}\gamma_{\lambda c'}}{E_{\lambda} - E} + R_{\text{background}}$$

Levels observed in data

Infinite number of higher lying levels

$$R_{cc'} = \sum_{\lambda} \frac{\gamma_{\lambda c}\gamma_{\lambda c'}}{E_{\lambda} - E} + \left(\frac{\gamma_{\lambda c}\gamma_{\lambda c'}}{E_{\lambda} - E}\right)_{\text{background}}$$

In practice, one often just uses one "background level" (per $J^{\pi}$)

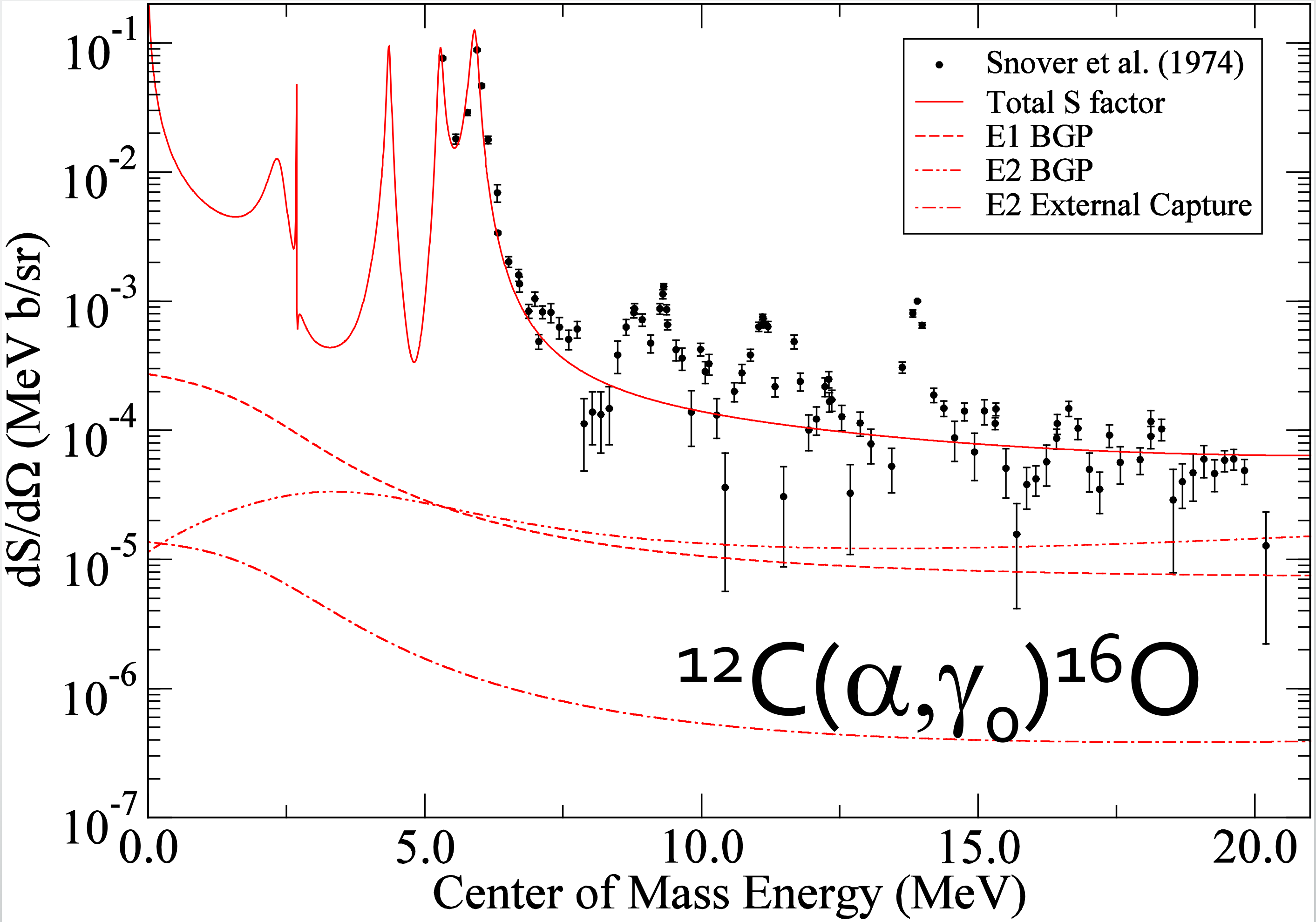

Best solution: Fit experimental data up in energy until the cross section gets smaller or there is a natural gap in the level structure.

# Fit to higher energy

- Challenges
  - Multiple particle decay channels
  - Multiple entrance channel data
- Additional advantages
  - Combine $^{12}$C($\alpha,\gamma$), $^{15}$N($p,\gamma$), and $^{15}$N($p,\alpha$) R-matrix analyses into single consistent analysis
  - Check on systematic uncertainties like effective energy determination and partial width consistency

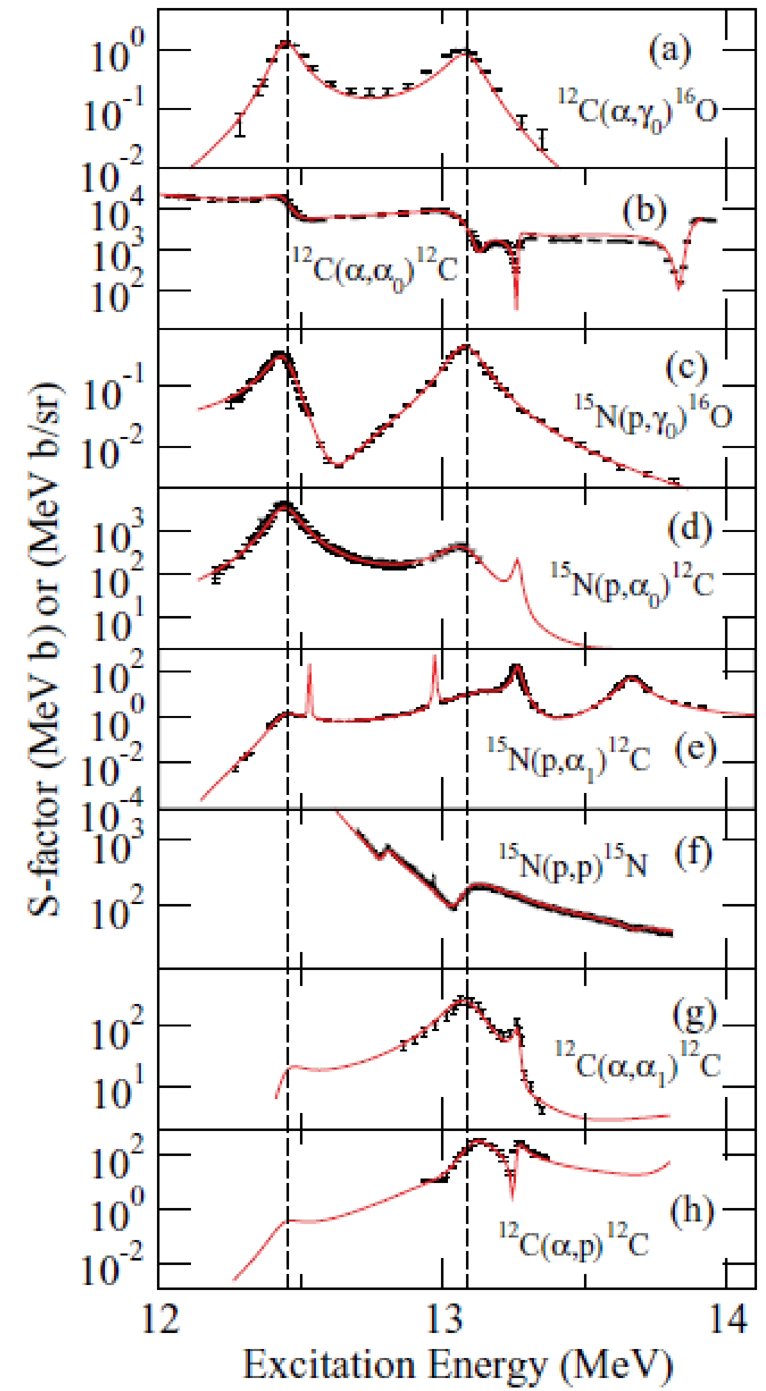

# *R*-matrix LEGO blocks (reaction components)

- **Resonance**
- **Subthreshold state**
- **HS External Capture**

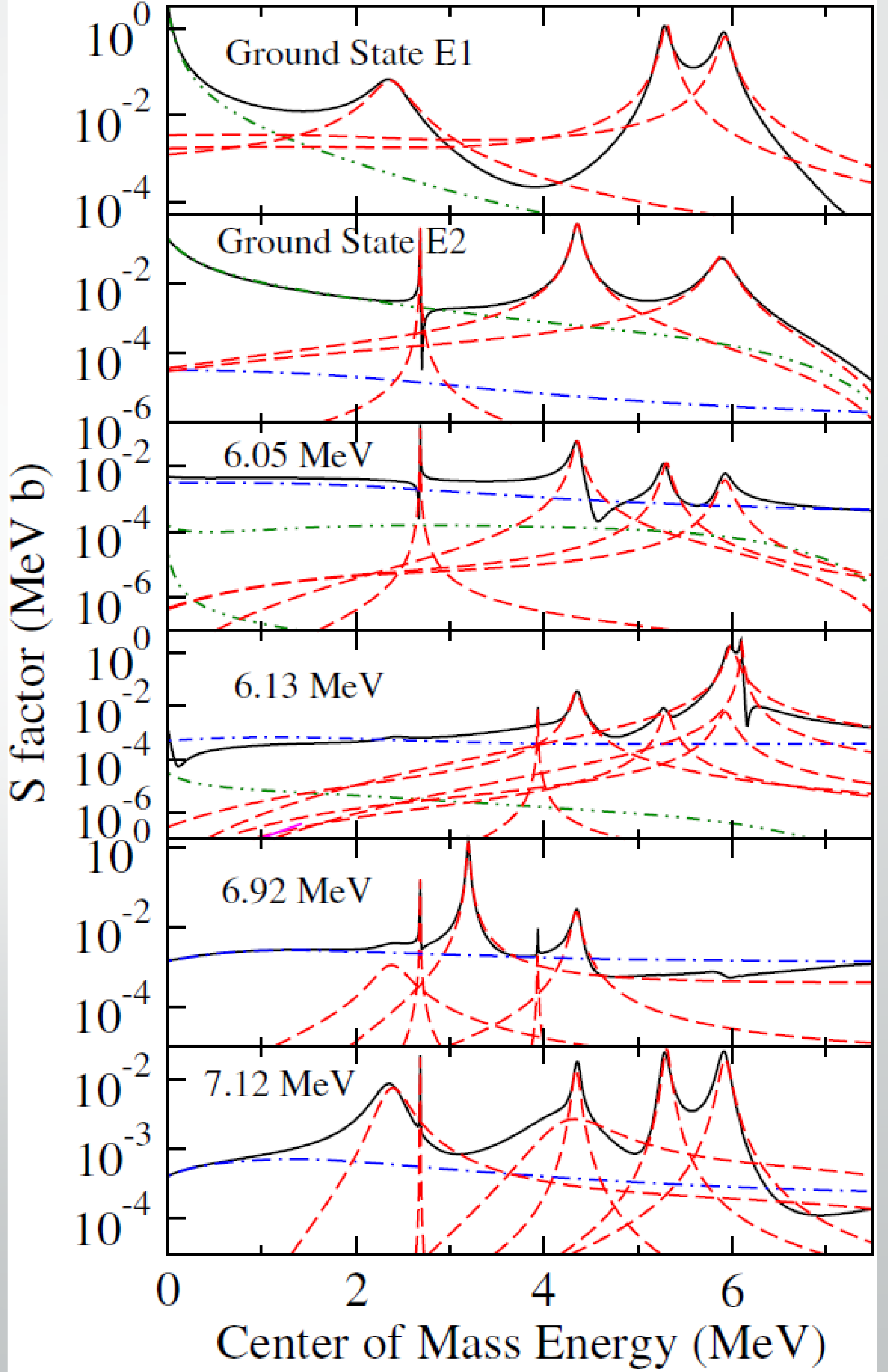

# “E1 and E2” data

- Can in principle measure the “E1 cross section” by measuring the differential cross section at 90 degrees.
  - Problems when E2 >> E1
- To get E2 one needs to measure the angular distribution.
- Main issue: often only the E1 and E2 derived cross sections have been reported in the literature, and the original angular distributions are omitted.
- Problems with extracting E2 data
  - Number of parameters to use for fit.
  - Systematic problems with data
  - Can often be corrected/understood if original angular distribution data are given
  - See Brune and Sayre (2013)

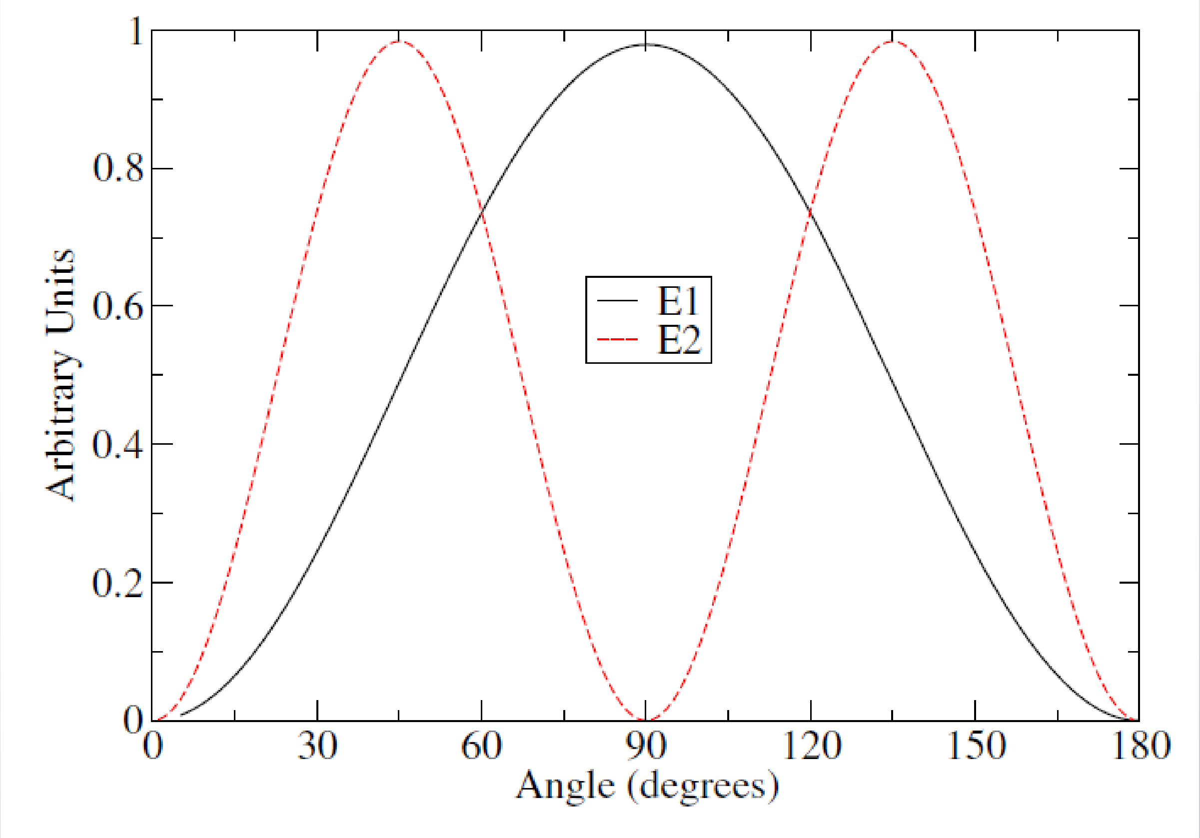

# Measurement Highlights: High Precision $^{12}C(\alpha,\gamma)^{16}O$ low energy measurements

- Makii et al. (2009)
- Used **time-of-flight** to separate out background from $(n,\gamma)$ reactions produced by neutrons from the $^{13}C(\alpha,n)^{16}O$ reaction
- Only two energies, but **highly accurate and precise**
- Just wish they could have done more measurements

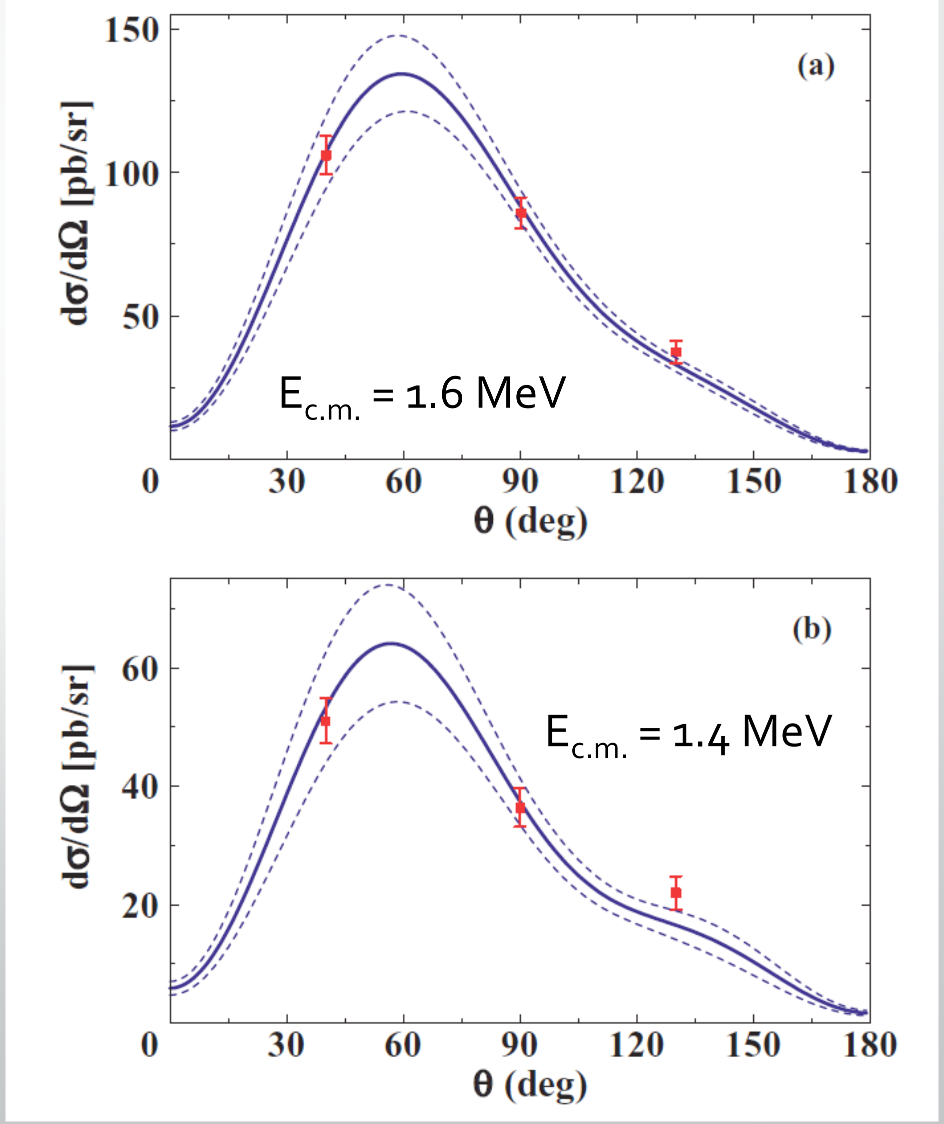

# ANCs: Strength of subthreshold states and external capture

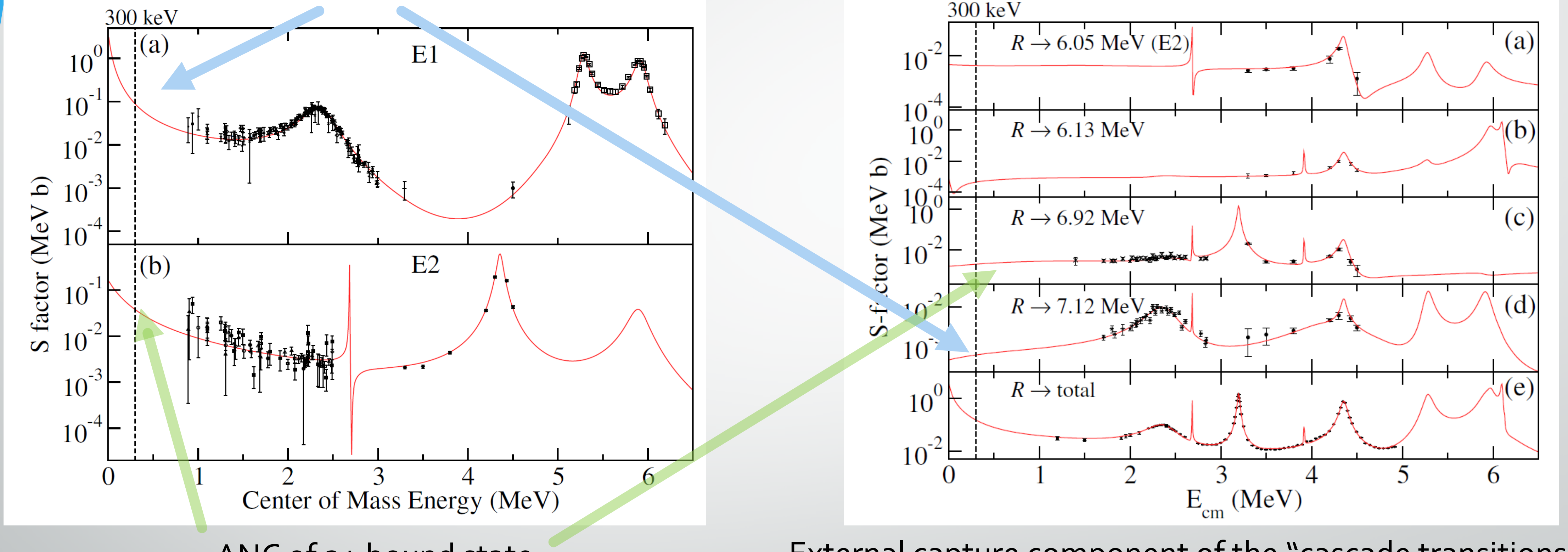

ANC of bound state 1⁻

ANC of 2+ bound state

Subthreshold states for the ground state transitions ($1^-$ and $2^+$)

External capture component of the “cascade transitions”

$$T_p^J(\mathrm{ext}) = -2i\boldsymbol{\Omega}\boldsymbol{P}^{1/2}k_\gamma^{L+1/2} \times \{\boldsymbol{P}^{-1}\boldsymbol{x}+[\boldsymbol{I}-\boldsymbol{R}(\boldsymbol{L}-\boldsymbol{B})]^{-1}\boldsymbol{R}(\boldsymbol{y}+i\boldsymbol{x})\}$$

$$= -2i\boldsymbol{\Omega}\boldsymbol{P}^{1/2}k_\gamma^{L+1/2}[\boldsymbol{I}-\boldsymbol{R}(\boldsymbol{L}-\boldsymbol{B})]^{-1} \times \{[\boldsymbol{I}-\boldsymbol{R}(\boldsymbol{L}-\boldsymbol{B})]\boldsymbol{P}^{-1}\boldsymbol{x}+\boldsymbol{R}(\boldsymbol{y}+i\boldsymbol{x})\}.$$

$$R_{cc'} = \sum_\lambda \frac{\gamma_{\lambda c}\gamma_{\lambda c'}}{E_\lambda - E}, \quad \boxed{C_{\lambda c}} = \frac{(2\mu_\alpha a_c)^{1/2}}{\hbar W_c(a_c)} \frac{\tilde{\gamma}_{\lambda c}}{[1+\sum_{c'}\tilde{\gamma}^2_{\lambda c'}(dS_{c'}/dE)(\tilde{E}_\lambda)]^{1/2}},$$

$$x_c = \sum_{l_f} \frac{\bar{e}^L_\alpha}{\hbar}(\mu_\alpha a_c)^{1/2} V(Ll_fJs;lJ_f)\boxed{C_{\alpha s l_f}} J'_{cl_fL} \quad y_c = \sum_{l_f} \frac{\bar{e}^L_\alpha}{\hbar}(\mu_\alpha a_c)^{1/2} V(Ll_fJs;lJ_f)\boxed{C_{\alpha s l_f}} J''_{cl_fL}.$$